Letter of Transmittal

Aidan Topping, Technical Communications Instructor
University of Manitoba SB-332
97 Dafoe Rd
Winnipeg, Manitoba

Dear Aidan,

We are writing you regarding Team 25's final report for the MECH 4860 Capstone course titled "*CNG Rack Lightweighting with composites*". This project was sponsored by New Flyer Industries with the main contact being Mark Townsley, C.E.T. The purpose of this report is to detail all the analysis and design of the project, as well as overview the assembly of the final product and give an estimated cost. We'd like to thank you for your technical communications feedback throughout the course and look forward to your feedback pertaining to this project.

Sincerely,

Team 25
Robin Armstrong
Harmanpreet Kaur Smagh
Mel Christopher Nirza
Tianyi Zhang

Bus Riders Consulting

CNG Rack Lightweighting with Composites

Final Design Report

Team 25

MECH 4860: Engineering Design
Submitted: December 5th, 2019

Prepared for:

- Paul Labossiere
- Mark Townsley

Prepared by:

Robin Armstrong _____

Mel Christopher Nirza _____

Harmanpreet Kaur Smagh _____

Tianyi Zhang _____

Executive Summary

This report outlines the design changes of a structural steel rack that holds tanks containing compressed natural gas (CNG), for the purpose of weight reduction and ease of assembly. The CNG rack is mounted on the roof of New Flyer's transit buses, therefore weight reduction was requested by the client, namely *New Flyer Industries* (NFI). The team, *Bus Riders Consulting*, was successful in achieving the needs of the client having gone through analysis of the rack and making required design changes.

To achieve weight reduction, the team intends to replace the main structural steel beams of the rack frame with glass fibre reinforced polymer (GFRP) 2x2 inch square tubes with a ¼" wall thickness. An aluminium sheet panel that spans along the rack will be replaced with a sandwich structure panel comprised of GFRP skin and Balsa core. To achieve an easier assembly of the frame, the team intends to change four joints (corner nodes) that connect the perimeter beams with a die-cast Aluminum 6061-T6 corner node, in which the beams can be slotted into, bolted, and bonded with ease. The new single piece corner node alleviates the need of welding together multiple steel pieces to join beams.

The existing total weight of the parts in scope amounted to 223.3 lbs. The total weight of the new parts totals to 124.6 lbs. With the changes implemented, a 44% weight reduction of the overall rack will be achieved.

Table of Contents

List of Figures

List of Tables

1 Introduction

This report focuses on the final design recommended by Bus Riders Consulting regarding a weight reduction project requested by New Flyer Industries. The report will provide the project background and considerations, then detail all engineering work performed by Bus Riders Consulting regarding the project. A prototype manufacturing plan will be given with an estimated cost.

1.1 Client Background

New Flyer Industries (NFI) is the largest transit bus and motor coach manufacturer in North America. NFI has been in operation for over 85 years and the facility in Winnipeg produces more than 2,000 transit buses, and 600 coaches yearly. They currently support over 105,000 buses and coaches worldwide, with their popular product line being the Xcelsior models. In recent years, the interest towards alternative fuel has grown. Vehicles that are more fuel efficient and friendlier towards the environment are being sought out. As a result, development in alternative fuels has been prioritized by NFI. Such alternative fuels being used by the New Flyer fleet are hydrogen fuel cell, diesel electric hybrid, full electric, and compressed natural gas (CNG).

1.2 Problem Statement

New Flyer Industries has requested the services of Bus Riders Consulting to analyze their current Compressed Natural Gas (CNG) racks to look for opportunities to reduce weight in the assembly. The current racks are comprised entirely of structural steel, are overdesigned, and heavier than they need to be.

1.3 Problem Scope

This project will involve the research of alternative materials to replace the current structural members in the CNG rack. TABLE I covers the areas of the rack which are in scope for this project, the objective of each area, as well as the methods to be used by Bus Riders Consulting in order to achieve the required objectives.

TABLE I: RACK AREAS IN-SCOPE

Rack Area	Objective	Method
Front Beam	Material Replacement	Material Research Static Stress Analysis FEA Validation
Side Beam	Material Replacement	Material Research Static Stress Analysis FEA Validation
Center Beam	Material Replacement	Material Research Static Stress Analysis FEA Validation
Walkway Pad	Material Replacement	Material Research Static Stress Analysis FEA Validation
Walkway Structure	Part Removal	Static Stress Analysis
Corner Nodes	Re-Design	Static Stress Analysis FEA Validation

An overview of a single CNG rack assembly and these components can be seen in Figure 1.

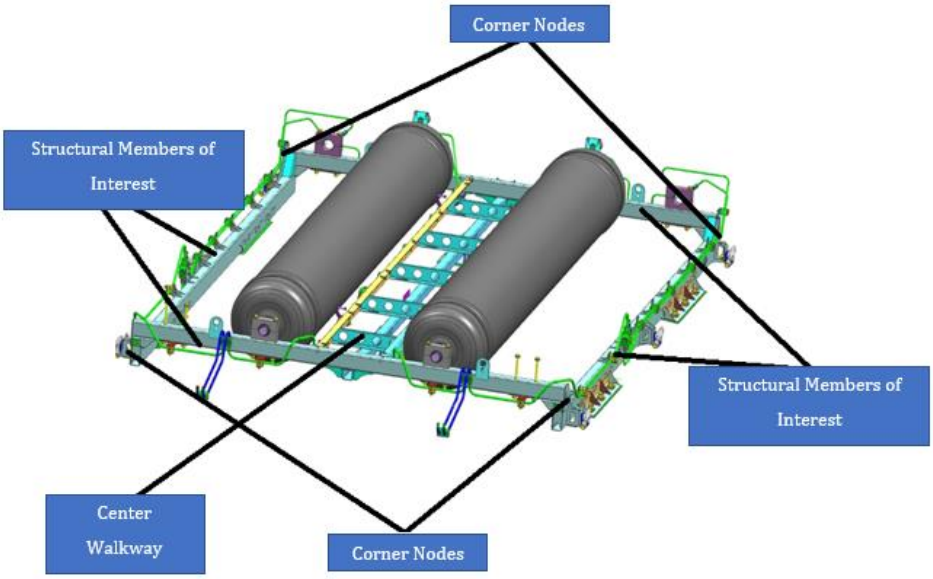

Figure 1: Existing CNG rack

Each New Flyer bus has at minimum two CNG rack assemblies on the roof, so any changes to a component will result in double the weight savings.

2 Project Overview

The client needs and requirements guide the project and place limitations on possible designs and materials which can be used. This section of the report will detail the needs of the client as well as discuss constraints and limitations affecting the project.

2.1 Client Needs

A list of needs was generated to guide design and material decisions based on meetings with the client. Each need was given a priority number with five being the highest priority and one being the lowest. Each need pertains to the redesigned CNG rack. For example, need one would be "The redesigned CNG rack must be lighter than the existing CNG rack". These needs can be seen in TABLE II.

TABLE II: PROJECT NEEDS

#	NEED	Imp
1	Must be lighter than the existing CNG rack.	5
2	Must have the same layout as the existing CNG rack.	5
3	Must have same mounting points to the roof as the existing CNG rack.	5
4	Promises a lifespan of at least 25 years.	5
5	Can be easily maintained.	5
6	Must be able to support the same load as the existing CNG rack.	5
7	Must maintain the same functionality as the existing one.	4

Since the project will not result in a new product, it is crucial that the design matches the functionality of the existing CNG rack. This is shown in needs #2, #3, #6, and #7 in TABLE II. As such these needs will be used to justify possible design decisions which may be made in order to reduce weight in the rack.

2.2 Current State Weight Breakdown

At present, each CNG rack assembly shown in Figure 1 weighs 1320 lbs. This weight includes all structural members as well as the weight of the actual CNG tanks (of which there are four per rack). TABLE III summarizes the weights of each section.

TABLE III: WEIGHT BREAKDOWN

Category	Weight [LBS]	% of Total
Hardware	186.97	14.17%
Valving	50.35	3.81%
CNG Tanks	652.2	49.41%
Rack Doors	88.39	6.70%
Structural	341.97	25.91%
	1319.88	100.00%

The area which is being targeted for weight reduction is the structural components, which is currently 341 lbs or 25.91% of the overall CNG rack assembly weight.

2.3 Project Constraints

As this project is a University student project, there are several constraints outside the control of Bus Riders Consulting which may have an impact on the process and final result of the project. These constraints are listed in TABLE IV.

TABLE IV: PROJECT CONSTRAINTS

Constraint	Description
Timeline	The project is limited to three months
Prototype	Due to budget, no prototype can be made
Testing	Due to lack of prototype, no physical testing can be done
Student Licenses	Limit on the number of nodes available for ANSYS FEA

3 Concept Selection

This section will detail the concept and designs which were selected by Bus Rider's Consulting to be further analyzed and given a detailed design.

3.1 Beam Material

The current material in use for the structural beams is AISI 1018 steel. For the loading on the rack, this material is heavy and over-designed, and replacement with a lighter material will improve bus performance. Materials considered for the structural beams were required to be lightweight with a good strength-to-weight ratio. Composite materials such as carbon fiber and glass fiber polymers were considered, as well as lightweight alloys such as magnesium and aluminum. Each material considered was given a ranking between one and six (with six being the best score) for various criteria and scored based on this ranking. The highest scoring material was then selected. The decision matrix used for this determination can be seen in TABLE V.

TABLE V: BEAM MATERIAL WDM

		Weight of Criteria								
Material		Customer (%)	Quality (%)	Cost (%)	Testing (%)	Manufacturing (%)	Weight (%)	Lifecycle (%)	Total Score	Rank
CFRP	Rating out of 6	3	6	1	1	6	6	2	3.53571429	4
	Score	0.10714286	0.428571429	0.178571429	0.17857143	0.857142857	1.5	0.285714286		
GFRP	Rating out of 6	3	5	5	1	6	5	6	4.5	1
	Score	0.10714286	0.357142857	0.892857143	0.17857143	0.857142857	1.25	0.857142857		
Magnesium AM50	Rating out of 6	3	3	3	2	2	4	3	2.92857143	6
	Score	0.10714286	0.214285714	0.535714286	0.35714286	0.285714286	1	0.428571429		
Magnesium AM60	Rating out of 6	3	4	3	2	2	4	3	3	5
	Score	0.10714286	0.285714286	0.535714286	0.35714286	0.285714286	1	0.428571429		
Aluminium 6061	Rating out of 6	3	3	6	6	4	2	4	4.10714286	2
	Score	0.10714286	0.214285714	1.071428571	1.07142857	0.571428571	0.5	0.571428571		
Aluminium 6063	Rating out of 6	3	1	6	6	4	2	4	3.96428571	3
	Score	0.10714286	0.071428571	1.071428571	1.07142857	0.571428571	0.5	0.571428571		

Based on the material research as well as the rectangular cross section of the current beams, Bus Riders Consulting determined that a glass fiber reinforced polymer (GFRP) would achieve the best balance of structural requirements, ease of manufacturing, and weight reduction from steel.

The most effective form of manufacturing for glass fiber beams with this cross section is known as pultrusion. To ensure feasibility of this method, various manufacturers were contacted regarding their ability to provide New Flyer with the proper materials. It was determined that while material cost of pultrusion is low, utilizing a custom die would be excessively expensive ($10,000 USD per die). As such, Creative Pultrusions will be selected as the source for the pultruded beams, as they offer off the shelf cross sections [1]. This will limit the possible cross section to a 2"x2" square beam, with a ¼" wall thickness.

3.2 Corner Node Concept

Presently, the beams are jointed at the corners of the rack by several gussets and tubes welded to the steel beams. This can be seen in Figure 2.

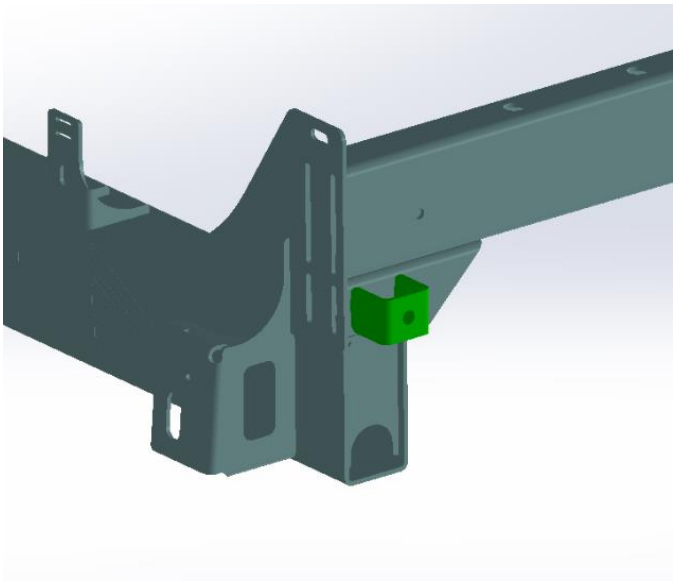

Figure 2: Current corner node design

Due to the replacement of steel with GFRP, a new jointing method is required. A single corner node piece will reduce the number of parts in the rack and allow for jointing of the beams in such a way to maintain their mounting point locations. Various designs were considered, and the top concept was selected in the same method as the beam material. The decision matrix for this can be seen in TABLE VI.

TABLE VI: CORNER NODE WDM

		Weight of Criteria								
Material		**Customer (%)**	**Quality (%)**	**Cost (%)**	**Testing (%)**	**Manufacturing (%)**	**Weight (%)**	**Lifecycle (%)**	**Total Score**	**Rank**
Folded Plate	Rating out of 6	3	1	6	4	5	5	1	4.07142857	2
	Score	0.107143	0.071428571	1.071428571	0.714286	0.714285714	1.25	0.142857143		
Column Beam Slot	Rating out of 6	3	3	2	3	2	3	3	2.67857143	5
	Score	0.107143	0.214285714	0.357142857	0.535714	0.285714286	0.75	0.428571429		
Tapered Beam Slot	Rating out of 6	3	4	1	3	1	2	4	2.32142857	6
	Score	0.107143	0.285714286	0.178571429	0.535714	0.142857143	0.5	0.571428571		
One Piece Flange Neck	Rating out of 6	3	6	4	3	4	4	6	4.21428571	1
	Score	0.107143	0.428571429	0.714285714	0.535714	0.571428571	1	0.857142857		
One Piece Neck	Rating out of 6	3	2	4	3	4	4	2	3.35714286	3
	Score	0.107143	0.142857143	0.714285714	0.535714	0.571428571	1	0.285714286		
Collar	Rating out of 6	3	2	5	2	3	4	1	3.07142857	4
	Score	0.107143	0.142857143	0.892857143	0.357143	0.428571429	1	0.142857143		

Bus Riders Consulting determined that the "One Piece Flange Neck" would be the most effective design to capture all requirements of the corner node. The preliminary design of this concept can be seen in Figure 3.

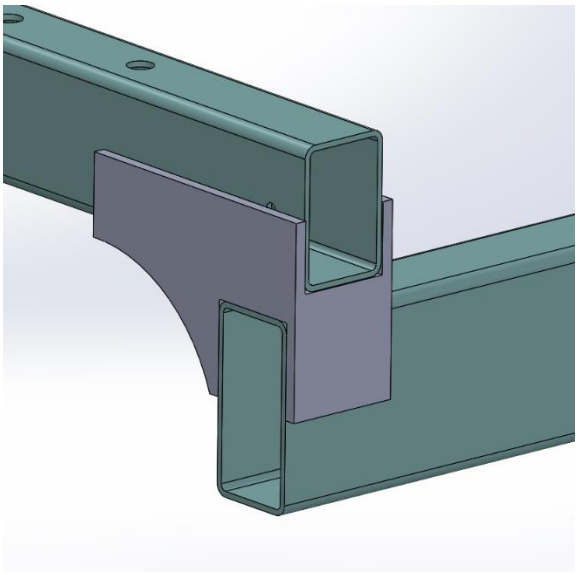

Figure 3: Preliminary corner node design

Based on the geometry of this concept, the material to be used in its construction will be Aluminum 6061-T6. This is due to its high strength-to-weight ratio, as well as the ability to either die cast or 3D print complex shapes in the manufacturing of the node. This will allow for complex geometries to be designed.

3.3 Walkway Concept

The walkway of the CNG rack consists one center beam, two L-beams and a walkway panel which lies on the L-beams. The redesign of the walkway is focusing on the walkway panel and the center beam, as the L-beams are not significantly heavy and support the tubing of the rack.

The current walkway panel is made of aluminum with the dimension of 126in X 14in and has a weight of 20lbs. The design is constrained by the maximum deflection, which is not allowed to exceed $\frac{1}{16}$ in. In this project, the aluminum walkway panel will be replaced by a composite sandwich panel and different material combinations have been tested in order to find the optimum material combination. The new sandwich panel will maintain the same size of the current design, but the thickness will be changed depending on the detailed design of the sandwich structure. The detailed analysis of the walkway panel is completed in Section 6 Walkway Analysis.

4 Beam Analysis

The first section of the CNG rack to be discussed are the structural beams. These beams comprise most of the structural weight and thus altering the material to be lighter will have a large impact on the overall weight reduction. The team's approach to analyse the beams are as follows:

- Obtain reaction forces of beams through hand calculations
    - A worst-case scenario of 300 lbs applied on beams and walkway was assumed through the analysis. The 300 lbs accounts for a person standing on the CNG rack.
- Validate the use of FEA simulation with hand calculated results
- Use hand calculated applied loads and reaction forces as conditions for FEA
- Observe the FEA results of GFRP beams
- Determine the weight reduction of the GFRP beams from the existing design.
- Indicate any recommendations based on the FEA results of GFRP beams.

Each step of the approach will be outlined further in detail in the following subsections.

4.1 Hand Calculation of Beams

To ensure success in our beam design, careful steps must be done for our analysis of the beam that will support various loads. The analysis began with taking note of all applied loads and their locations on the beam as well as locations of fixed supports of the existing design. With this, hand calculations were done with the assumption of point loads and supports.

4.1.1 Front Beam

Figure 4 shows the applied loads on the front beam which are the CNG tanks. The front beam is supported by the side beams on either end, and the center beam in the middle. Each tank weighs 161 lbs and is carried by two front beams (one at each end). As such, the tanks' loads were halved which becomes a load of 358 N. All the applied loads were taken as point loads. There is also a load applied by the walkway onto the centre of the beam, however this load is directly on the centre fixed support, thus for simplicity the load was ignored for now.

Figure 4: Front view of the front beam

It was observed that the loading scenario of the beam was symmetrical, thus the front beam was halved for further hand calculations. Figure 5 shows the FBD of the halved beam and since the beam is halved, only two loads and two fixed supports will be accounted in the hand calculations.

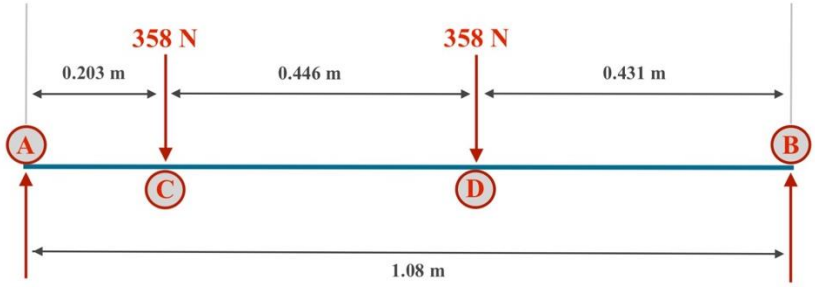

Figure 5: Free body diagram (FBD) of half of the beam.

Shown in Figure 5, the location of the forces and supports can be seen. Given this, the reaction forces at the supports can be determined using static equilibrium equations.

$$\sum F_y = 0 \qquad \textit{Equation 1}$$

$$F_A + F_B = F_C + F_D \qquad \textit{Equation 2}$$

It can be assumed that summation of all forces in the vertical direction must equal to zero due to static equilibrium. The unknown variables are F_A and F_B and these are the reaction forces at the supports that must be solved. Since there are two unknowns, Equations 3 and 4 was formed.

$$\sum M_A = 0$$ *Equation 3*

$$-(F_C)(AC) - (F_D)(AD) + (F_B)(AB) = 0$$

$$F_B = \frac{(F_C)(AC) + (F_D)(AD)}{(AB)}$$ *Equation 4*

It can be assumed that the summation of the moments about location A is zero due to static equilibrium, thus the reaction force at location B can be solved. With F_B known, F_A was calculated.

4.1.2 Centre Beam

The centre beam supports loads from the front beams and the walkway. Seen in Figure 6, the centre beam fixed supports and applied loads were simplified into point loads on an FBD. The 258 N force was a value previously obtained from the reaction force of the front beam fixed supports.

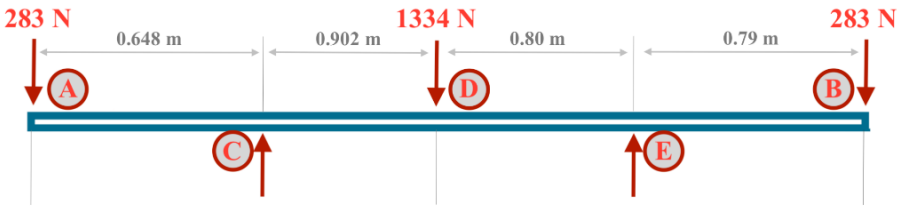

Figure 6: Free body diagram (FBD) of the centre beam

Shown in Figure 6 is the location of the forces and supports. In this loading case, the 300 lb force is located directly at the middle which is shown as 1334 N. Given this, the reaction forces at the supports can be determined using static equilibrium equations.

$$\sum F_y = 0$$ *Equation 5*

$$F_C + F_E = F_A + F_D + F_B \qquad \textit{Equation 6}$$

It can be assumed that summation of all forces in the vertical direction must equal to zero due to static equilibrium. The unknown variables are F_C and F_E and these are the reaction forces at the supports that must be solved. Since there are two unknowns, equation 7 and 8 were used.

$$\sum M_C = 0 \qquad \textit{Equation 7}$$

$$(F_A)(AC) - (F_D)(CD) + (F_E)(CE) - (F_B)(CB) = 0$$

$$F_E = \frac{(F_D)(CD) + (F_B)(CB) - (F_A)(AC)}{(CE)} \qquad \textit{Equation 8}$$

Another loading case however is when the 300 lbs is at the end of the centre beam, where the front beam is located. The FBD of this case is shown in Figure 7.

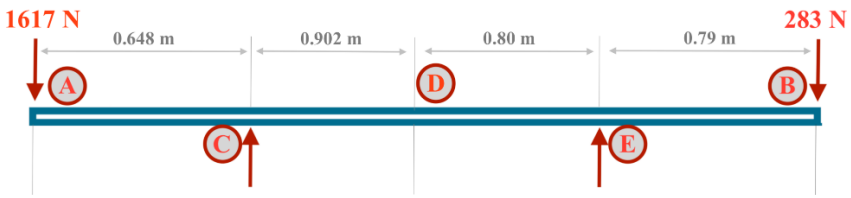

Figure 7: Free body diagram (FBD) of the centre beam with 300 lbs applied at the end

For this case, the following moment equation was used instead.

$$F_E = \frac{(F_B)(CB) - (F_A)(AC)}{(CE)} \qquad \textit{Equation 9}$$

It can be assumed that the summation of the moments about location C is zero due to static equilibrium, thus the reaction force at location E can be solved using equation 9. With F_E known, F_C was calculated.

4.1.3 Side Beam

Like the centre beam, the side beams provide support for the front beams as well as act the connection for the overall rack to the roof of the bus. Seen in Figure 8, the side beam fixed supports and applied loads were simplified into point loads on an FBD. The 433 N force was a value previously obtained from the reaction force of the front beam fixed supports.

Figure 8: Free body diagram (FBD) of the side beam.

The locations of fixed supports and applied loads are shown in Figure 8. With this, the summation of the forces in the y-direction (vertical) on the beam was equaled to zero due to static equilibrium. The following equations represents this assumption.

$$\sum F_y = 0 \qquad \textit{Equation 10}$$

$$F_C + F_D = F_A + F_B \qquad \textit{Equation 11}$$

The unknown variables are F_C and F_D and these are the reaction forces at the supports that must be solved. To solve for the two unknowns, equations 12 and 13 were formed with the assumption of static equilibrium.

$$\sum M_C = 0 \qquad \textit{Equation 12}$$

$$(F_A)(AC) + (F_D)(CD) - (F_B)(CB) = 0$$

$$F_D = \frac{(F_B)(CB) - (F_A)(AC)}{(CD)} \qquad \textit{Equation 13}$$

Equation 13 shows that the total moments about location C is zero, meaning that there is no rotation about C. With that, F_D can be calculated. With F_D known, the reaction force F_C can be determined.

4.1.4 Validity of Finite Element Analysis

It is necessary to confirm that the hand calculations results agreed with results obtained from FEA simulation. This is to ensure that further results obtained from FEA simulation were valid as the project became increasingly dependent on the use of ANSYS software. A way to validate was to compare the maximum bending stress result between hand calculations and FEA simulation.

To calculate the maximum bending stress, shear and moment diagrams were needed. From the moment diagram, the highest bending moment was recorded which was then used in the following equation to solve for $\sigma_{bending}$, the maximum bending stress.

$$\sigma_{bending} = \frac{(M)(y)}{I} \qquad \textit{Equation 14}$$

M	Bending moment [N.m]
y	Distance from the neutral axis to the surface [m]
I	Centroidal moment of inertia [m^4]
σ	Bending stress [Pa]

One of the beams, that being the front beam, was selected to be used for stress comparison. Using the values obtained from the front beam's FBD, its shear and moment diagrams were plotted, thus its maximum bending moment determined. Its maximum bending moment was then used to calculate the maximum bending stress value. This value was then compared to finite element analysis (FEA) simulation results using CAD models of the existing beam design. Once the hand calculated results and simulation results were compared to each other, a decision can be made if FEA simulation can be used for further analysis. The team observed that the calculated values were within 4% of the FEA results, and thus it was concluded that FEA simulation would be a reliable tool for further analysis of new designs.

4.1.5 Finite Element Analysis of GFRP Beams

Given the validity of FEA simulation, the next step was to perform simulation on the beam made of GFRP. Because the GFRP is a composite material, hand calculations would have been complicated, thus further analysis of parts made of GFRP was performed with FEA. In addition, since composites was dealt with, performing FEA simulation was more involved. In this case, ANSYS Composite PreACP was used in conjunction with static FEA simulation of ANSYS to account the behaviour of composite materials. In ACP, the beams were setup to match a 2"x 2" square beam with unidirectional glass fibres along the beam length given a thickness of 0.25" Full PreACP settings can be seen in Appendix D. The entirety of FEA simulation performed on the beams used the reaction forces obtained from hand calculations as conditions for fixed supports and applied loads. All loading conditions for the three beams analyzed are found in Appendix C

4.2 Front Beams

The purpose of the front beams is to act as the primary supports of the four CNG tanks that the rack will carry. These beams are directly connected to the CNG tank mounts meaning that careful consideration must be taken when designing the new beams. The layout of the CNG tanks cannot change. The mounts of the CNG tank attached to the front beam can be seen in Figure 9.

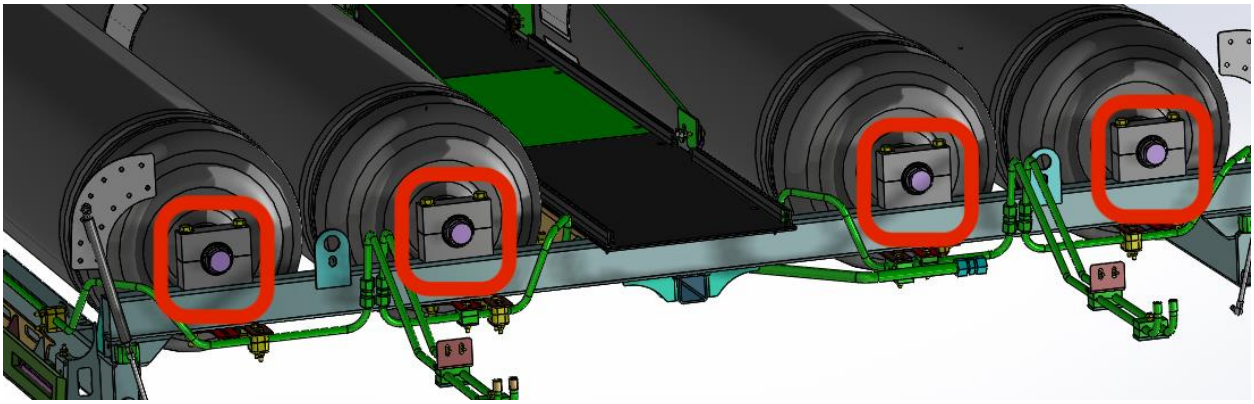

Figure 9: The front beam with cylindrical CNG tanks mounted

From Figure 9, vertical bolts run through the mounts and into the front beam to secure the CNG tanks as well as extend underneath the beam to provided attachments for tubing. These mounts must not be changed. With that, holes must run through the beam and must be kept at the same location for the new design.

4.2.1 Current Front Beam Design

The current front beam design is made from AISI 1018 steel. Figure 10 shows where the front beams are located on the CNG rack which are circled in red, as well as the location of the four CNG tanks (not to scale).

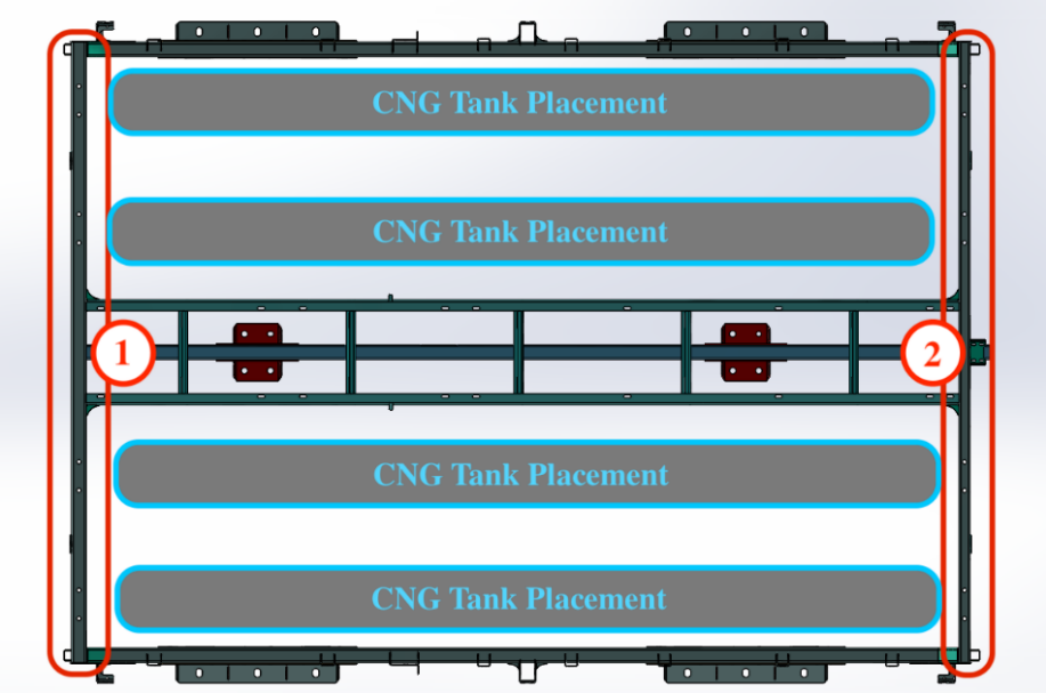

Figure 10: Top view of the current CNG rack design with front beams 1 and 2

The two front beams have almost the same dimensions except for their widths. TABLE VII shows the dimensions of the two beams. The reason for the different widths is that the front beam 1 and 2 have different amounts of attachments and fittings.

TABLE VII: OLD DIMENSIONS OF FRONT BEAMS 1 AND 2

Front Beam	1	2
Height	3 in	3 in
Width	2 in	1.5 in
Length	85 in	85 in
Thickness	0.125 in	0.125 in

The front beams have some major features that must not be changed, that being the mounting points on the beam where the CNG tanks will be attached. These mounting points are the holes where bolts will be put through and this can be seen Figure 11 and Figure 12. The hole sizes and positions will be kept the same for the new design so that the layout of the tanks is maintained.

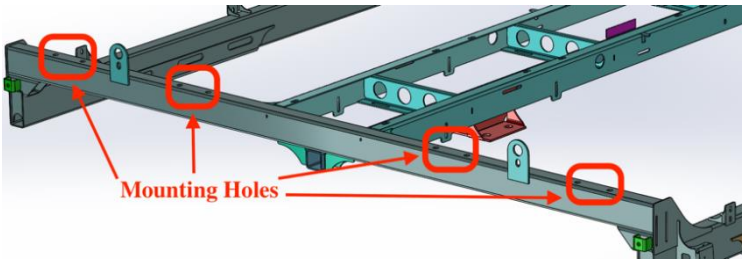

Figure 11: Mounting hole locations on the front beam

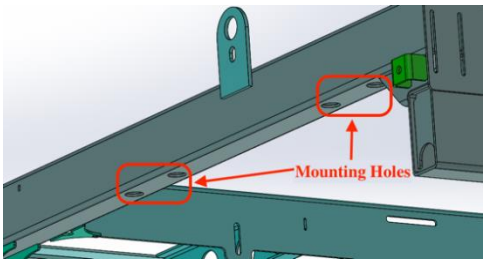

Figure 12: Underside of the front beam

Given the current dimensions and features of the front beams, it is essential for the new design to have these aspects the same to ensure that attachments such as the mounts of the CNG tank and of course, the tank itself be able to fit.

4.2.2 Results

This section outlines the results obtained through FEA simulation, and since the front beam was selected for FEA validity, the results from hand calculations will also be presented. This section also provides some discussion on what was observed from the various results.

Having gone through the hand calculations using the previously outlined method, the following results were obtained seen in

TABLE VIII.

TABLE VIII: RESULTS FROM HAND CALCULATIONS

Variable	Result
$\mathbf{F_A}$	433 [N]
$\mathbf{F_B}$	283 [N]
Largest bending moment	87.9 [N.m]
$\boldsymbol{\sigma_{bending}}$	5.65 [MPa]

With that, the hand calculated bending stress of 5.65 MPa was then compared to the bending stress obtained from the FEA simulation of the halved front beam.

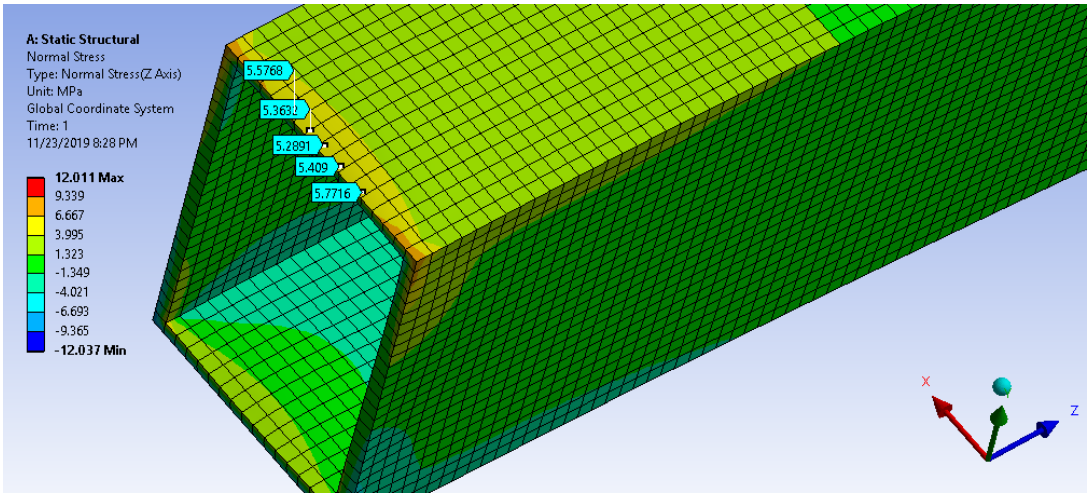

Figure 13: Bending stress observed from FEA simulation

The result presented in Figure 13 shows various stress values probed on the top surface of the beam, and it has similarities to the bending stress result obtained from the hand calculation which is 5.65 MPa. The bending stress on FEA simulation was determined by obtaining the normal stress experienced by the beam along its length, which is the z-axis in this case. The FEA stress average was found to be 5.48 MPa based on the five probed stress values. Because of the closeness of FEA results to 5.65 MPa with a difference of 3%, it was decided that FEA simulation would be used for further analysis of beam design. This satisfies the 4% error specified previously.

Having validated FEA for further analysis, Figure 14 shows the stress (von Mises) on the GFRP front beam. The simulation was done with the worst-case loading scenario of having a 300 lb load from the walkway directly on top of the front beam, as well as the applied loads of the four CNG tanks.

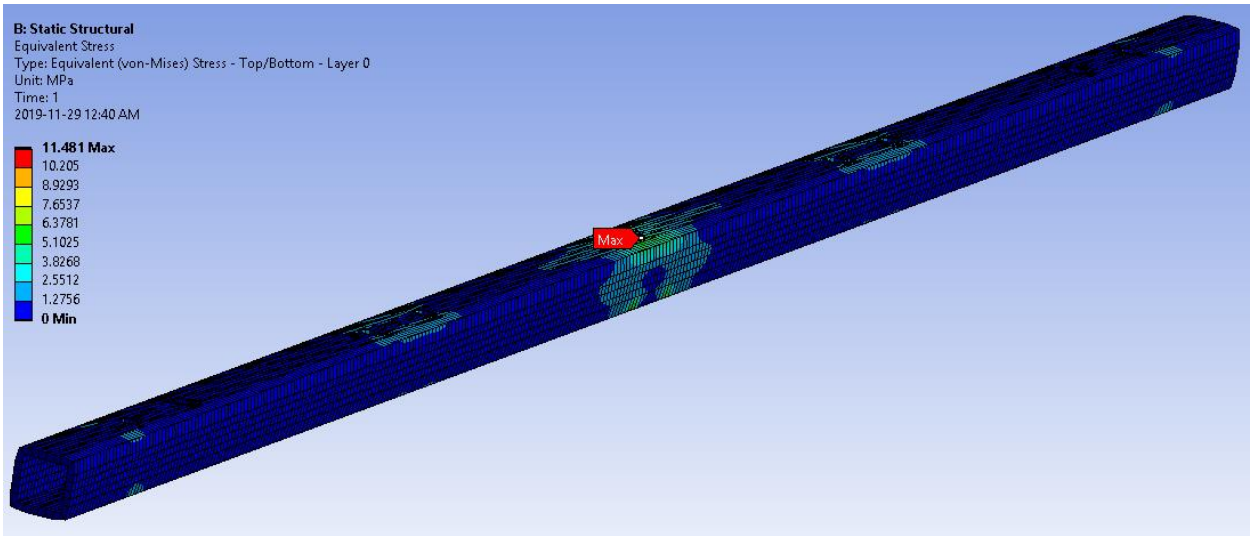

Figure 14: FEA simulation of the GFRP front beam

From Figure 14, the maximum stress is 11.5 MPa and is located at the hole at the top of the beam where a bolt will be inserted to join to the centre beam. 11.5 MPa was reached after having gone through a convergence study which be outlined further in this section.

The stress is highest at the middle of the entire beam since the loading scenario involves having the 300 lb load directly on top of the front beam. Figure 15 and Figure 16 show a closer look at the location of maximum stress.

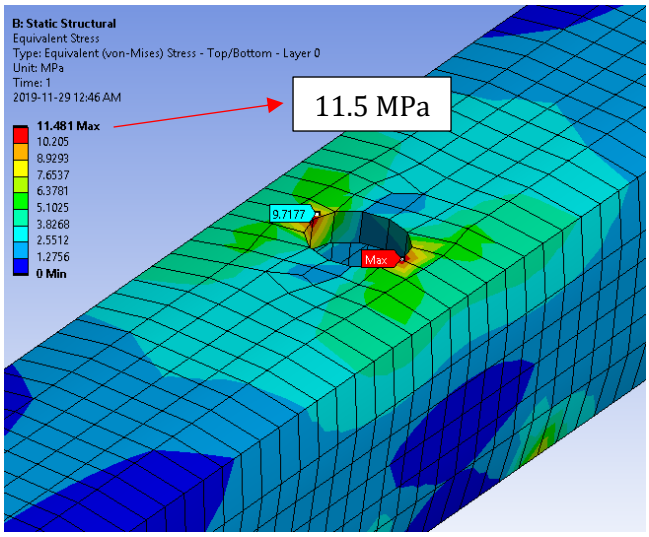

Figure 15: Max stress at the centre hole of the front beam

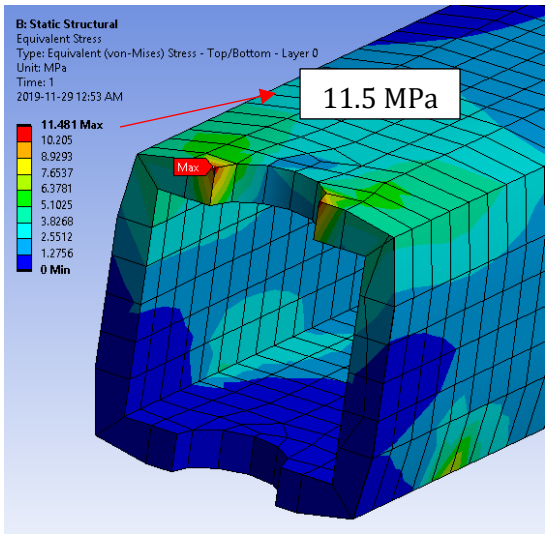

Figure 16: Cross-section of the middle of the beam

Another location where relatively high stress occurs is underneath the middle section of the beam. The stresses at this location can be seen in Figure 17 and Figure 18.

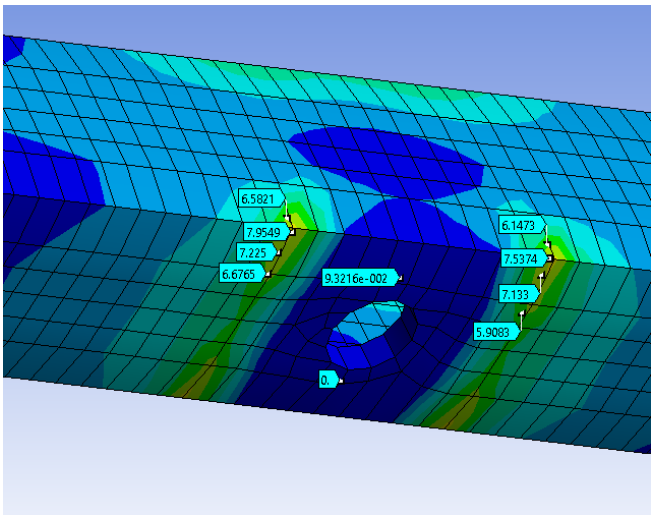

Figure 17: Stresses underneath the middle section of the beam

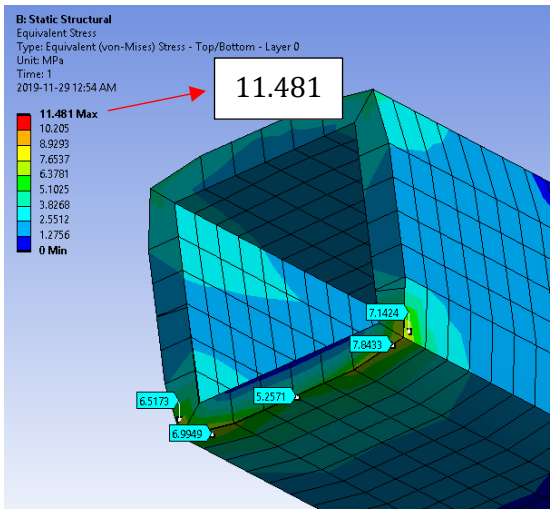

Figure 18: Cross-section of beam

Underneath the middle section of the front beam is the centre beam. It is seen in Figure 17 that there is an abrupt change in stress. The area of low stress is the contact point of the front beam and the centre beam. The higher stress area is at the edge of the centre beam, where the connection between the front beam and centre beam ends.

The FEA simulation was repeated to ensure accurate results. With each repetition, the quality of the mesh was increased, which is represented by the increase in the number of nodes. Appendix B shows a plot of the convergence study.

The maximum stress of 11.5 MPa is within the 30% yield of the beam to be sourced from Creative Pultrusions which has a maximum allowable stress of 16,500 psi (113.7MPa) [2].

Using GFRP instead of AISI 1018 achieves considerable weight reduction and this is shown in TABLE IX.

TABLE IX: WEIGHT REDUCTION OF FRONT BEAMS

Material	Beam Weight	
	Beam 1 (2 in width)	Beam 2 (1.5 width)
AISI 1018	29.5 lbs	25.2 lbs
GFRP	14.5 lbs	
Weight Savings	51%	42%

4.3 Side Beams

Like the front beam, the side beams are currently made from AISI 1018 steel. Figure 19 shows the location of the beams on the rack.

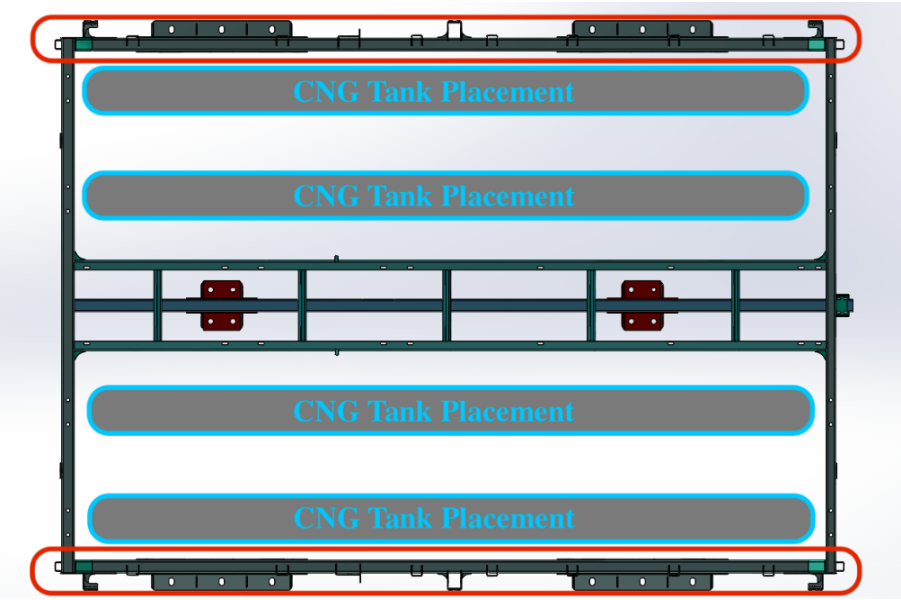

Figure 19: Top view of the current CNG rack design with side beams circled in red

The side beams are identical, with their dimensions being summarized in TABLE X.

TABLE X: SIDE BEAM DIMENSIONS

Side Beam	Dimensions
Height	4 in
Width	2 in
Length	123.25 in
Thickness	0.125 in

The side beams function cannot change due to client needs. They act as the supports for the front beams as well as mount the footpads which secure the CNG rack to the roof of the bus. A series of mounts for clamps holding thin diameter stainless steel tubes sit along the beams. The locations of these features can be seen Figure 20.

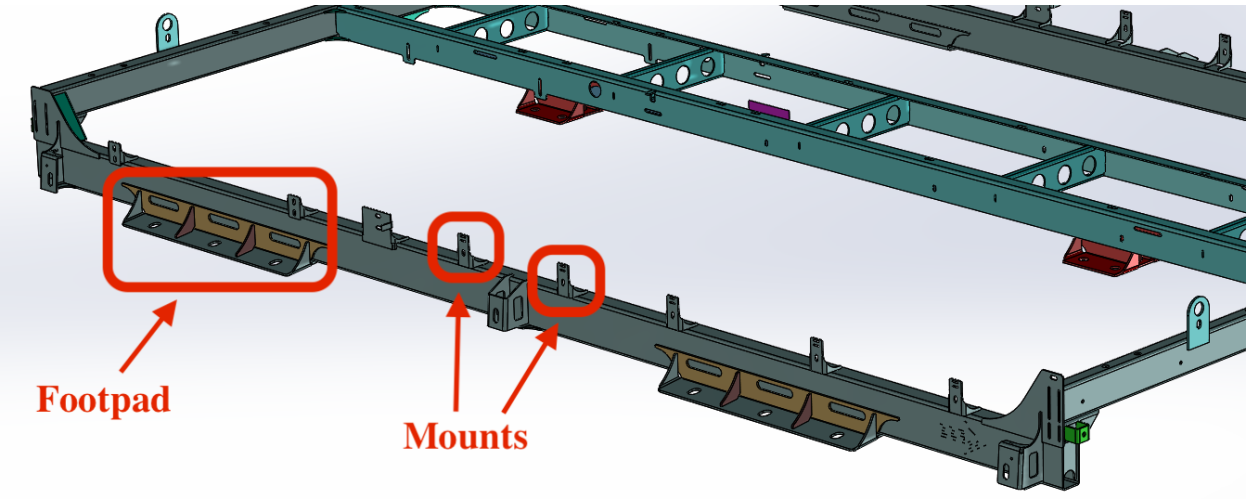

Figure 20: Features of the side beam

4.3.1 Results

Having done the FEA simulation, the maximum stress resulted to 14.9 MPa which is located at one of the holes for the footpad. This value was reached after going through a convergence study, which is shown in Appendix B. Figure 21 shows the von Mises stress of the GFRP side beam through FEA.

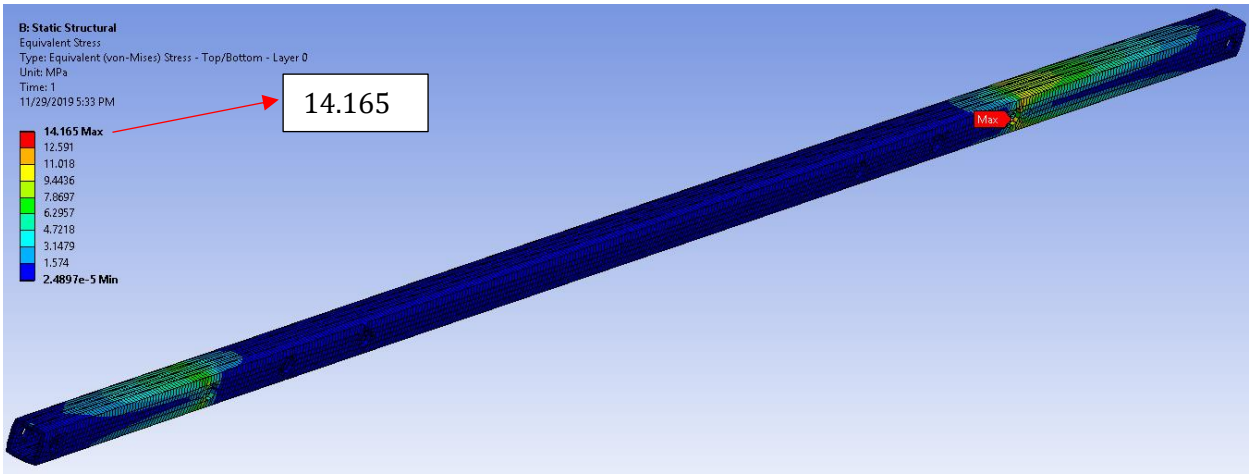

Figure 21: FEA simulation of the GFRP side beam

Since the location of the maximum stress is at the through-hole for the footpad connection, it is where the propagation of cracks is likely to occur. Figure 22 and Figure 23 show a closer look at the maximum stress location.

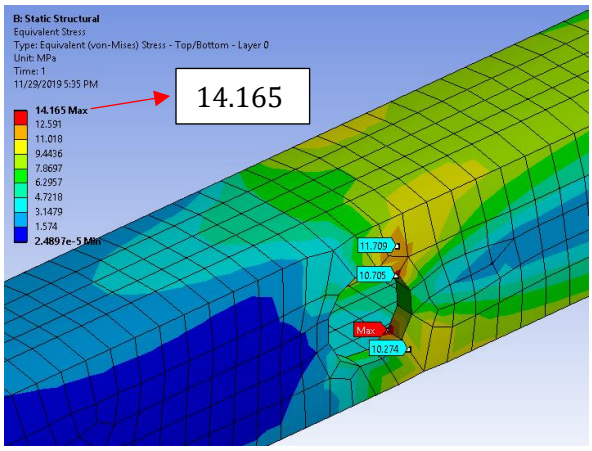

Figure 22: A closer view of the maximum stress location.

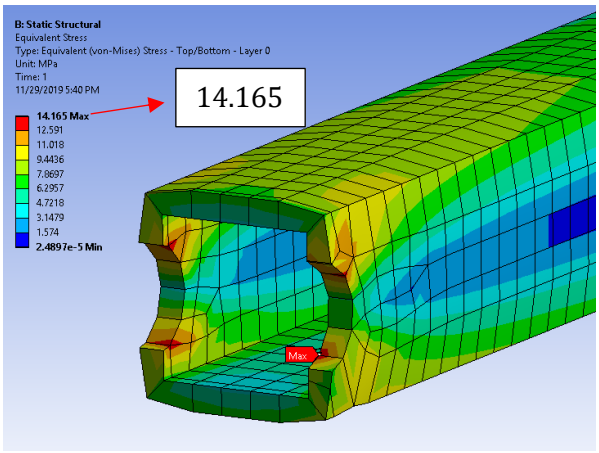

Figure 23: Cross-section of max stress location.

Each FEA simulation was repeated with increasing mesh resolution until the value of stress obtained from the results showed little variation. This can be seen in Appendix B where the maximum stress value converges to around 14 MPa. With the replacement of the current AISI 1018 side beams with GFRP 2x2 tube beams, there is considerable weight reduction. The amount of weight savings can be seen in TABLE XI.

The maximum stress of 14.2 MPa is within the 30% yield of the beam to be sourced from Creative Pultrusions which has a maximum allowable stress of 16,500 psi (113.7MPa) [2].

TABLE XI: WEIGHT REDUCTION OF SIDE BEAM

Material	Beam Weight
AISI 1018	48.9 lbs
GFRP	21 lbs
Weight Savings	57%

4.4 Center Beam

The centre beam plays a crucial role in that it supports the two front beams, supports the walkway, as well as provide a connection to the roof of the bus and the second rack. Like the side beams, the centre beam spans across the whole length of the rack. The centre beam is highlighted in blue in the whole rack assembly is shown in Figure 24.

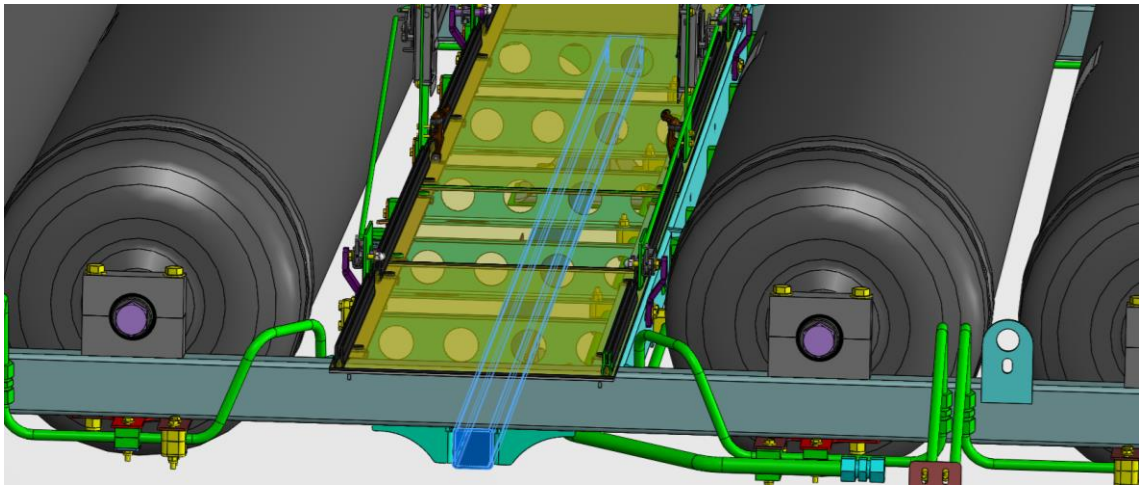

Figure 24: Centre beam placement in the CNG rack.

4.4.1 Existing Centre Beam Design

The current centre beam design is made from AISI 1018 steel. Figure 25 shows where the centre beam is located on the CNG rack which is circled in red, as well as the location of the four CNG tanks (not to scale).

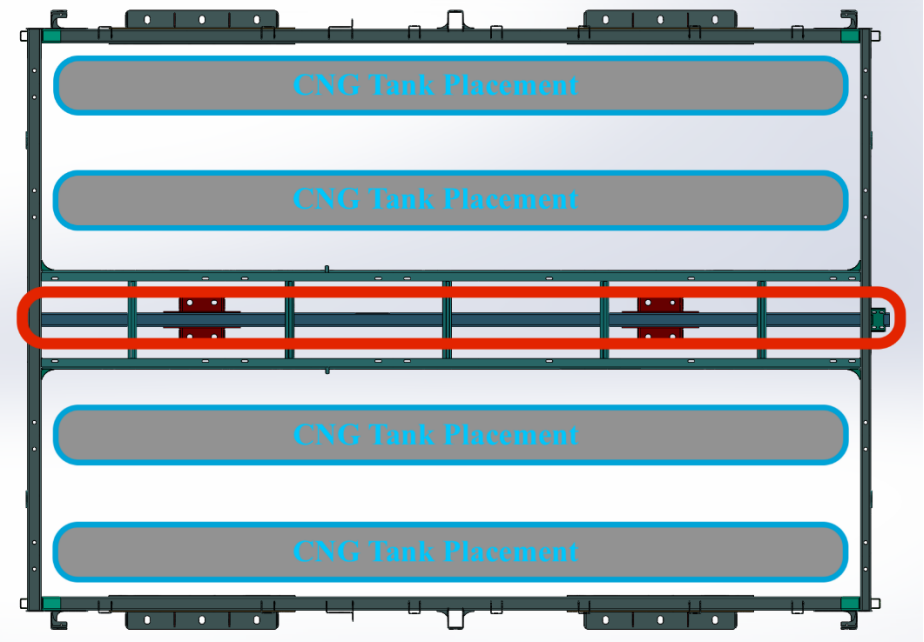

Figure 25: Top view of the current CNG rack design with centre beam circled in red.

As shown in Figure 25, the centre beam is placed under the five cross members and under where the walkway lies. The current dimensions of the centre beam can be seen in TABLE XII.

TABLE XII: CURRENT CENTRE BEAM DIMENSIONS

Centre Beam	Dimensions
Height	2 in
Width	2 in
Length	126 in
Thickness	0.125 in

At the end of the beam towards the right side, the centre beam extends out of the rack. This extension is what allows the connection for another CNG rack and is shown more closely in Figure 26.

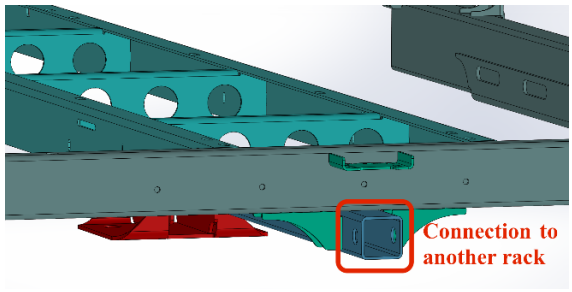

Figure 26: An extended end of the centre beam

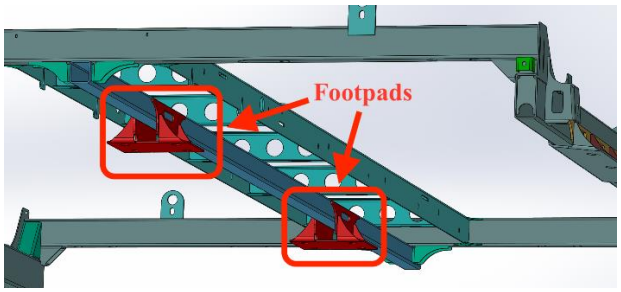

Figure 27: Footpads attached on the centre beam to mount onto the bus roof

As well as the extended end, another key feature of the centre beam are footpads seen in Figure 27. These footpads are what allow the whole rack to attach to the roof of the bus. The placement of these footpads along the centre beam was noted during the design of the new beam.

For the purpose of weight reduction, some cross members that are placed above the centre beam will be removed in the new rack design.

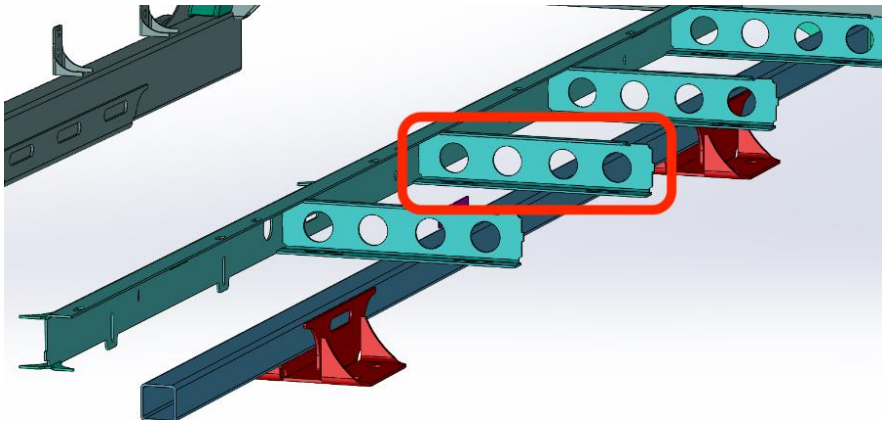

Figure 28: Circled in red is the cross member that will be kept for the new design

Seen in Figure 28, the cross member directly in the middle of the centre beam will be kept ensuring support between the walkway panel and the centre beam.

4.4.2 Results

Having done the FEA simulation, the maximum stress resulted to 36.42 MPa which is located at the middle of the beam where the single cross member is placed. This value was reached after going through a convergence study, which will be outlined further in this section. Figure 29 shows the von Mises stress of the GFRP centre beam through FEA.

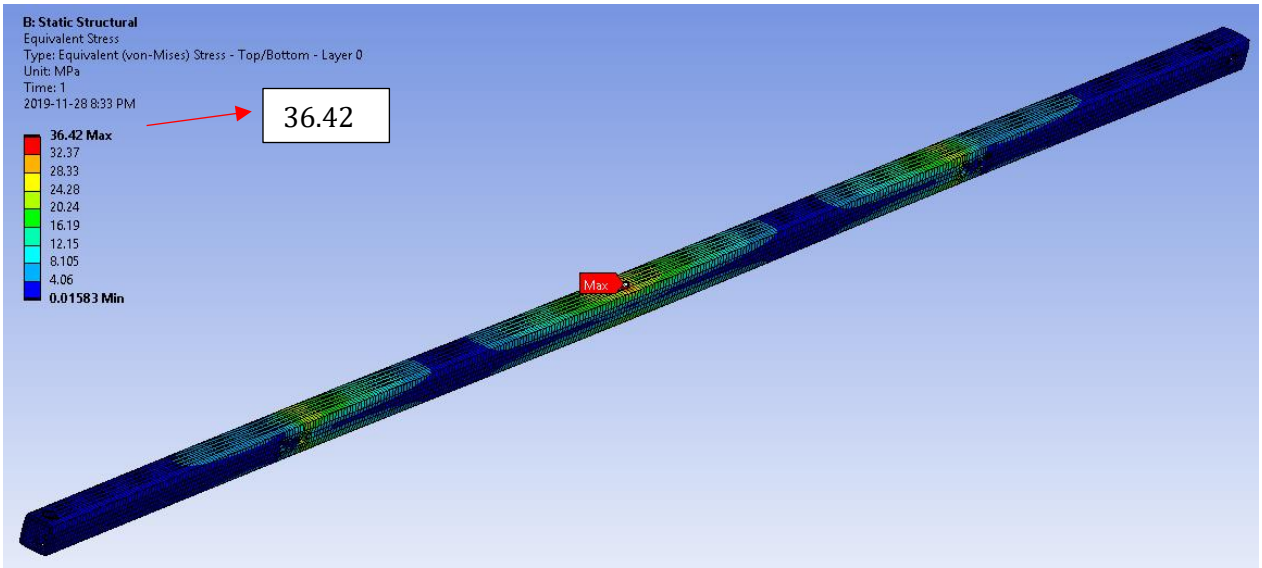

Figure 29: FEA simulation of the GFRP centre beam

The stress in the middle of the beam is high due the loading scenario of the 300 lb load being applied directly at the centre of the walkway. Figure 30 and Figure 31 show a closer look on the area where the single cross member will be placed. It can be seen that the stresses around the area range from 20 to 30 MPa.

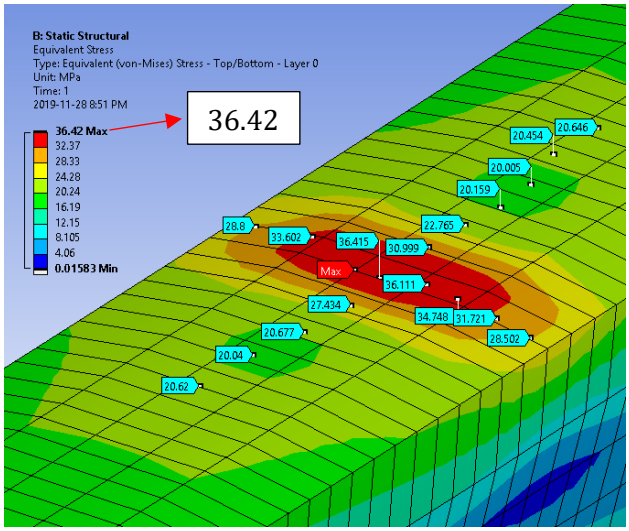

Figure 30: High stress area of the centre beam

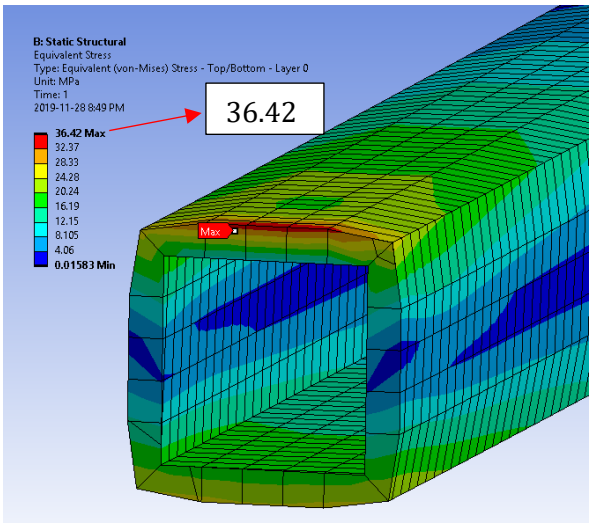

Figure 31: Cross section of the max stress location

Another area of relatively high stresses is at the holes where bolts will be placed to attach the footpads onto the beam. This is shown more closely in Figure 32 and Figure 33.

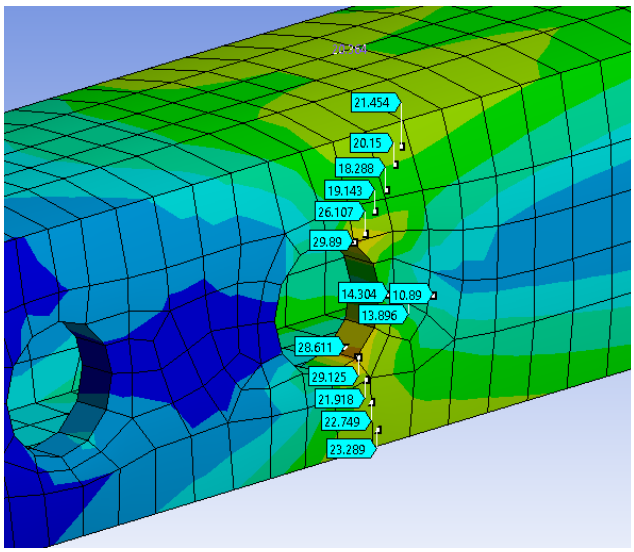

Figure 32: High stress at bolt holes of the centre beam

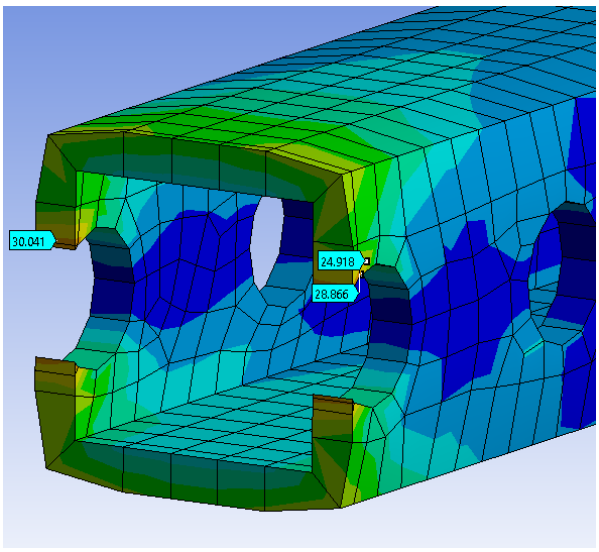

Figure 33: Cross-section cut at the bolt hole

Certain locations at the hole have stress concentrations, and these are the areas where the propagation of a crack is most likely to occur.

To ensure that the FEA results accurately simulated the stress on the beam, a convergence study was performed. This was done by increasing the resolution of the mesh of the model in ANSYS after every

simulation until the stresses observed in the results showed little variation. Appendix B shows the mesh convergence. The mesh converged at a maximum stress of 36.42 MPa, which is a reasonable result and that a higher mesh resolution is not needed to achieve more accuracy.

As well as stress, another factor to consider is the amount of deflection the beam will experience with the worst-case loading scenario. This was found to be a maximum of 3.58 mm and is shown in Figure 34.

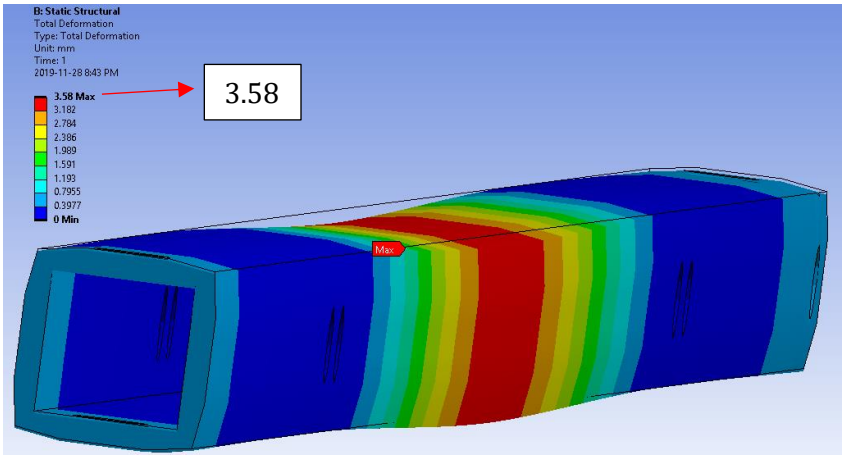

Figure 34: Maximum deformation of the centre beam

Figure 34 shows the true scale deformation of the beam. The wireframe of the undeformed beam is also shown for ease of comparison.

The maximum stress of 36.4 MPa is around the 30% yield of the beam to be sourced from Creative Pultrusions which has a maximum allowable stress of 16,500 psi (113.7MPa) [2]. This satisfies our goal of having the stress around 30% yield.

The weight savings of the center beam is seen in TABLE XIII.

TABLE XIII: WEIGHT REDUCTION OF CENTRE BEAM

Material	Beam Weight
AISI 1018	32.2 lbs
GFRP	21.7 lbs
Weight Savings	33 %

5 Corner Node Analysis

There are four corner nodes in each CNG rack, which serve to act as a joint for front and side beam. In the same area on the rack, there exists a mounting point for a hinge which the rack lid rotates about. Additionally, a gas spring for the lid is mounted at the same location. Due to the updated cross sections of the front and side beams, the corner node must be designed in a way to maintain the upper surface separation. This is important to all mounting points for the CNG tubes and roof mounting points are in the same location. This separation was determined to be 4.5 inches, as seen in Figure 35.

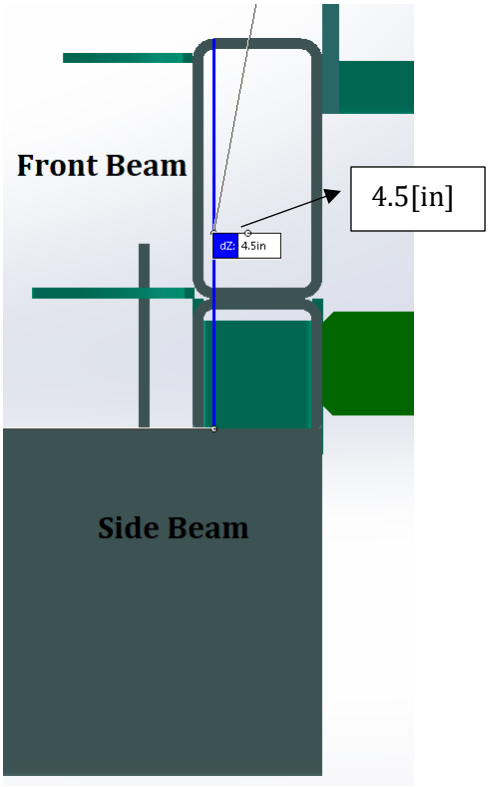

Figure 35: Beam separation

Jointing of the side and front beams to the corner node will be accomplished by a mix of bolted connections and epoxy between the beams and node. There is an additional constraint on the upper width of the corner node, as the locations of the CNG tank mounts prevent this dimension from exceeding four inches.

A design of the corner node based on these constraints was created and the design with dimensions can be seen in Figure 36.

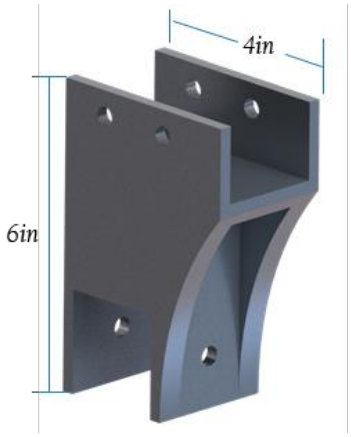

Figure 36: Corner node design

The separation of jointed faces in the node is 2.5 inches, which when combined with a two-inch height on the front beam meets the need of having 4.5 inches of separation. The load from the front beam to the side beam flows through the radius on the front of the design, and each beam is jointed using bolts as well as epoxy surface bonding.

5.1 Failure Analysis

Failure of the corner node is most likely to occur in the upper flanges jointing the front beam. During a braking event, the weight of the CNG tanks will be supported by this flange, so ensuring the structural performance of this area is required. As each front beam is symmetrical, this load will be supported by two corner nodes. The center beam joint will support some of this load and thus a beam analysis to determine the exact loads affecting the flange.

New Flyer defines an aggressive braking event at 0.3 G, so this will be the value used to determine the forces imparted from the CNG tanks. As each CNG tank is 75 KG, the force from each tank will be:

$$75 \times 0.3 \times 9.81 = 220 \text{ N}$$

The free body diagrams used in the analysis are seen in Figure 37 and Figure 38.

Figure 37: Load case for 0.3G braking event

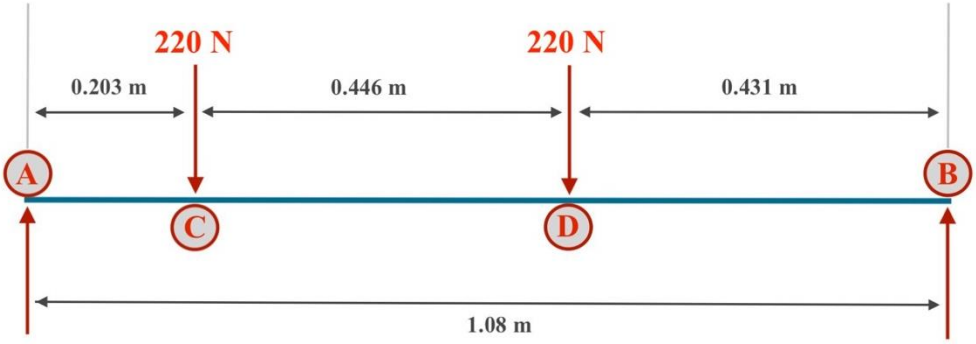

Figure 38: Reaction forces acting on the corner node flange

Therefore, the force acting on the flange is 178.14 N. To simplify analysis, the flange will be considered a cantilever beam with a distributed load across its surface. This can be seen in Figure 39.

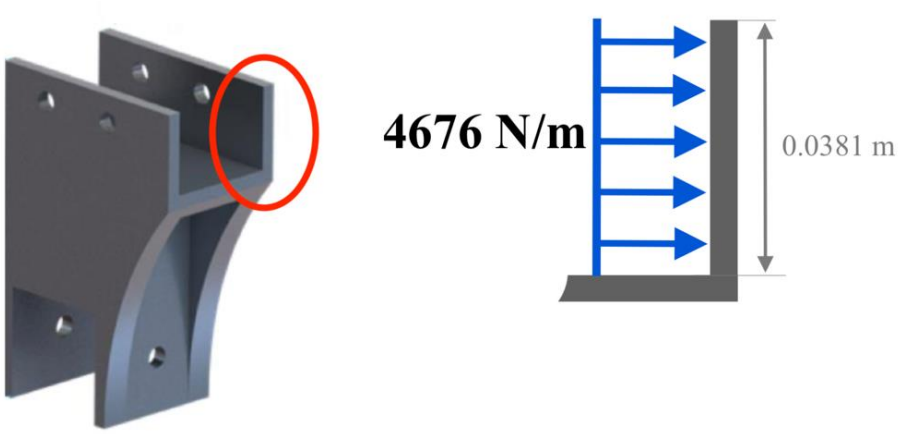

Figure 39: Simplified flange loading

Following beam deflection analysis and using the cross section of the flange the peak stress experienced by the corner node at this location is 4.97 mPa and the maximum deflection being 8.2E-6 meters. Therefore, the design will not fail during worst case loading and FEA will be used to validate the design further.

5.2 Finite Element Analysis

Two load cases will be used to perform FEA on the corner node, a stationary static loading analysis as well as a 0.3G braking event analysis to validate the previous results. Convergence plots were manually created by manually refining the mesh on each iteration and taking the maximum stress and deflection at each iteration, then plotting them until the stress and deflection converged to a value. The convergence plots for the corner node can be found in Appendix B.

5.2.1 Static Loading

Static loading of the corner node includes the front beam loading as well as the fixed support given by the side beam. For simplicity, it will be assumed that the inner faces of the side beam mounts will be fixed, and that the load translated from the front beam will be imparted to both the upper bolt holes and the upper flat face. The load from the front beam was calculated in Appendix A and is 433 N. Additionally, since the node is symmetrical the corner node will be halved along the plane of symmetry in order to allow for increased mesh refinement. Loading conditions are seen in Figure 40.

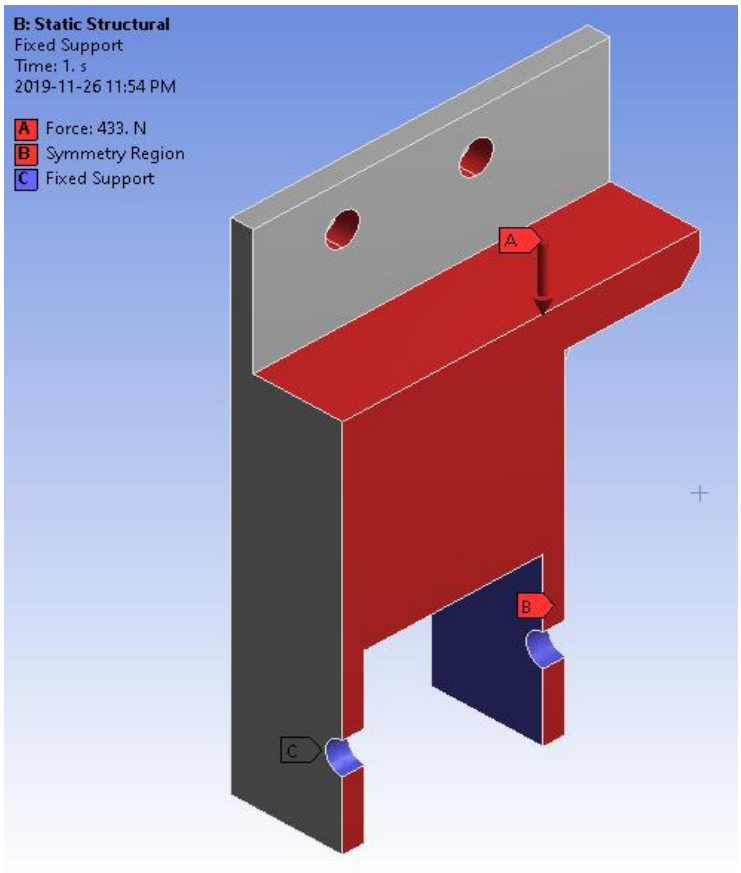

Figure 40: Corner node static loading conditions

The values of maximum stress and deflection converged after six iterations, with the maximum experienced stress being 1.12 mPa and the maximum deflection being 1.6E-6 m. These values are exceedingly lower than the maximum allowable stress and deflection in an aluminum 6061-T6 component, and thus the corner node is valid for static structural performance. The stress and deflection results from the final FEA iteration can be seen in Figure 41 and Figure 42 respectively.

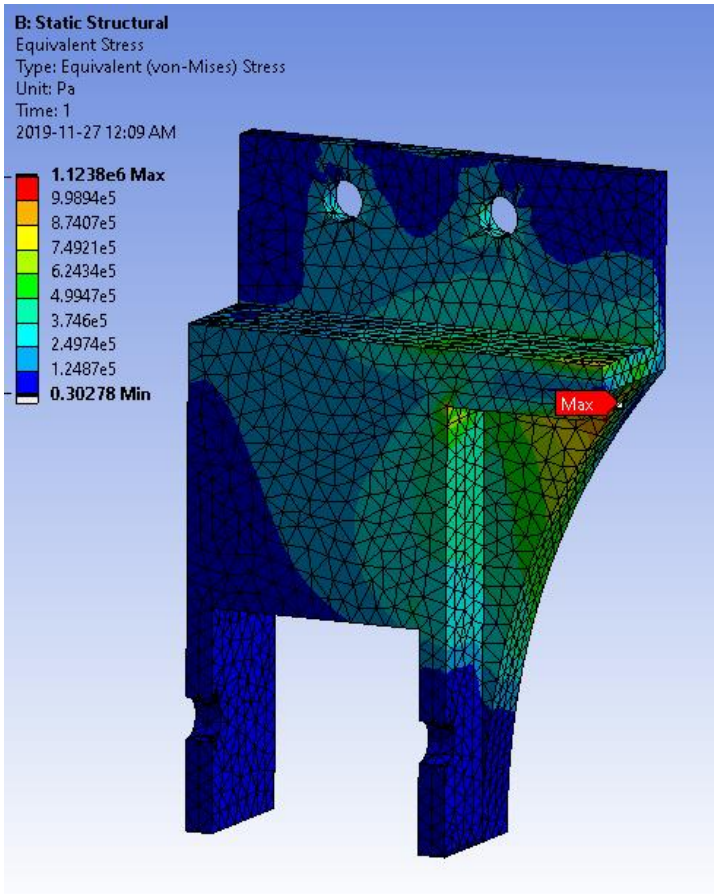

Figure 41: Corner node max static stress

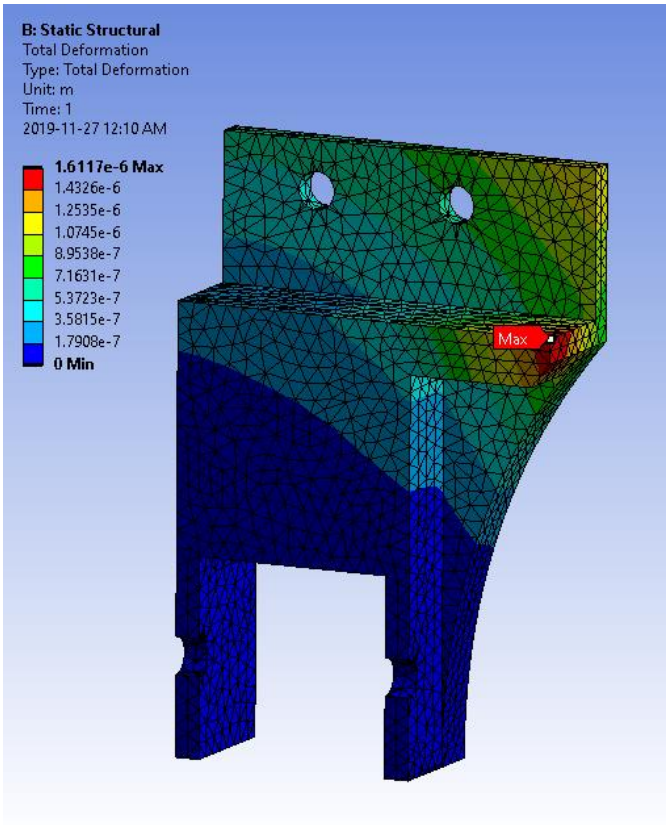

Figure 42: Corner node max deflection

5.2.2 Braking Event Analysis

As this analysis only affects the flange of the corner node, the model was simplified to allow for a more refined mesh and increase result accuracy. This simplified model as well as the loading conditions of the analysis can be seen in Figure 43.

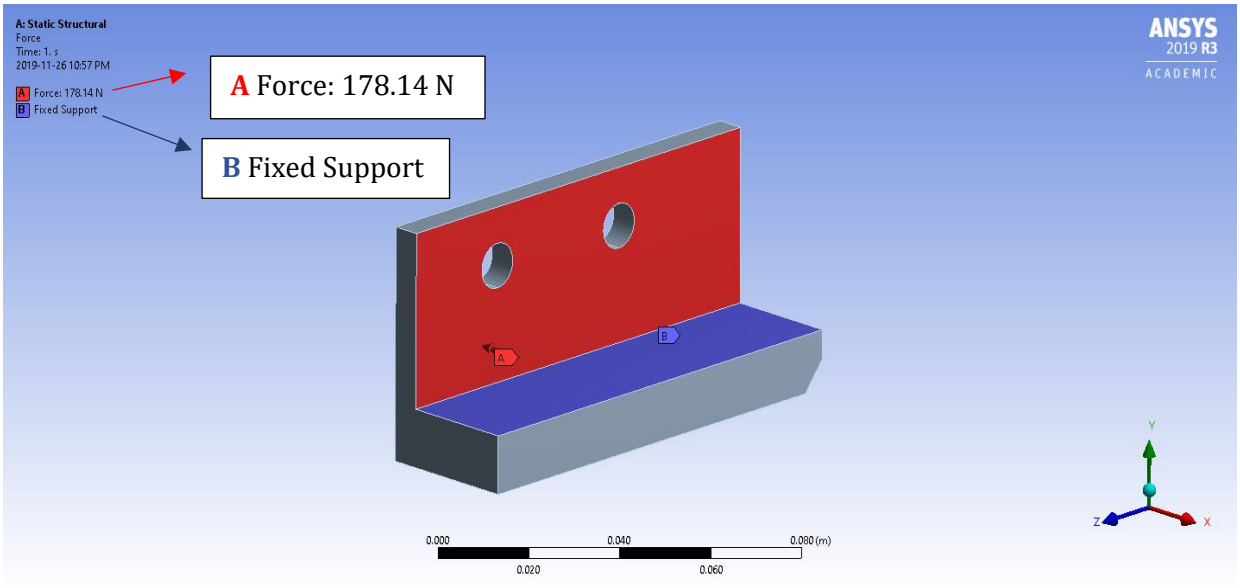

Figure 43: Braking event loading conditions

The values converged after six iterations as shown in Appendix B, with the final iteration maximum stress and deflection being shown in Figure 44 and Figure 45 respectively.

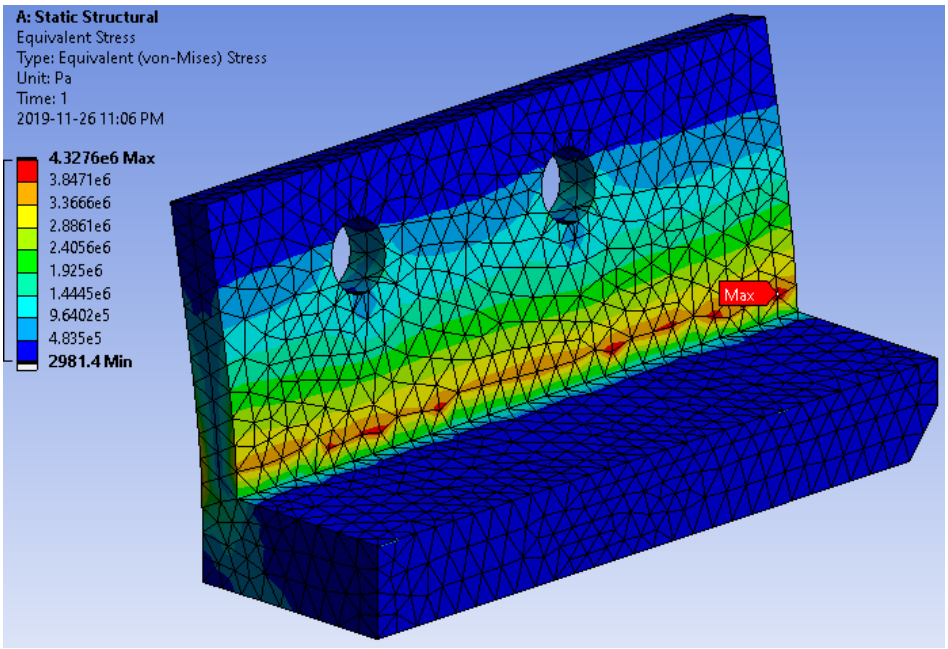

Figure 44: Maximum braking event stress

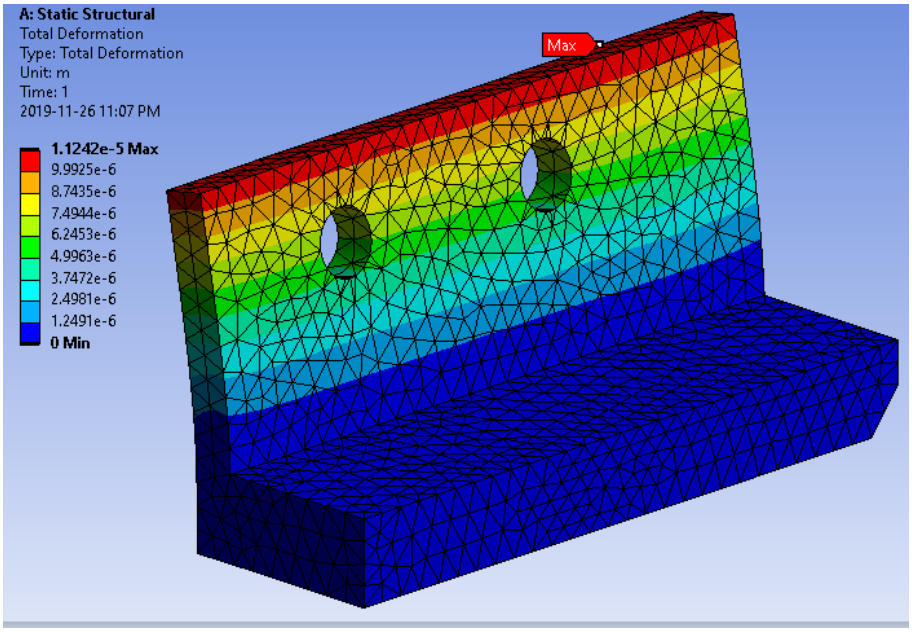

Figure 45: Maximum braking event deflection

A summary of the FEA results compared to the hand calculations can be seen in TABLE XIV.

TABLE XIV: FEA VS HAND CALCULATIONS CORNER NODE

	Hand Calculations	FEA	Percent Difference
Maximum Stress (mPa)	4.9	4.33	3%
Max Deflection (M)	8.23E-06	1.12E-05	8%

The percent difference between calculated values and FEA values for stress and deflection are 3% and 8% respectively. Therefore, the analysis is validated, and the corner node will not fail during a 0.3G braking event.

6 Walkway Analysis

In order to reduce the weight from CNG rack the walkway offers possibility in weight saving through replacing aluminum panels with the use of a composite sandwich panel. Four different type of sandwich structure were analyzed by Bus Riders Consulting. The loading of the walkway is translated into L-brackets which are mounted to the front beam. The three options of composite Sandwich described as following:

- Glass fiber – balsa – glass fiber
- Aluminum- foam - aluminum
- Carbon fiber- balsa – carbon fiber

The mechanical properties were calculated by using VectorLam [2]. Four different type of core and skin combinations available on VectorLam as shown in TABLE XV .

TABLE XV: POTENTIAL SANDWICH STRUCTURE COMBINATIONS AND MATERIALS

Sandwich structure	Available on VectorLam [2]
Glass fiber – balsa – glass fiber	E-EX1900-Baltek SB50- E-EX1900
Aluminum - foam - aluminum	6061 T6-Corecell A500- 6061 T6
Aluminum - foam – aluminum	6061 T6-Pxc.245- 6061 T6
Carbon fiber- balsa – carbon fiber	10.9oz Carbon cloth - Baltek SB50 - 10.9oz Carbon cloth

TABLE XVI present the properties of four options estimated through VectorLam.

TABLE XVI: ESTIMATED MECHANICAL PROPERTIES BY VECTOR LAM [2]

Material / Mechanical Properties	E-EX1900-Baltek SB50-E-EX1900	6061 T6-Corecell A500- 6061 T6	6061 T6-Pxc.245-6061 T6	10.9oz Carbon cloth-Baltek SB50-10.9oz Carbon cloth
E_f (Msi)	10.3	10	10	30
ρ_f (lb/in3)	0.092	0.098	0.098	0.065
ρ_s (lb/in3)	0.0034	0.0034	0.09	0.0034
E_c (Msi)	0.289	0.0093	0.08	0.289

The definitions of each symbol are shown in the TABLE XVII. Section 6.1 includes formulas for sandwich beam properties, material selection, detail design of walkway panel with design parameters. Further joint methods investigated for new walk and Fracture mode analysis and finite mode analysis performed on final design.

TABLE XVII: ILLUSTRATIONS OF EACH SYMBOL

Symbols	Definitions
$\boldsymbol{E_f}$	Elastic modulus of the skin material
$\boldsymbol{\rho_f}$	Density of the skin material.
$\boldsymbol{\rho_c}$	Density of the core material.
$\boldsymbol{E_c}$	Elastic modulus of the core material.

6.1 Formulas & Equations

The walkway design is constrained by the maximum deflection, which is defined by internal New Flyer specifications as $\frac{1}{16}$in. In order to design the dimensions of a sandwich structure, the following parameters need to be introduced: t is the thickness of the skin material, c is the thickness of the core, b is the width of sandwich beam, d is the total thickness and L is the length of the beam. Those parameters are illustrated in the Figure 46.

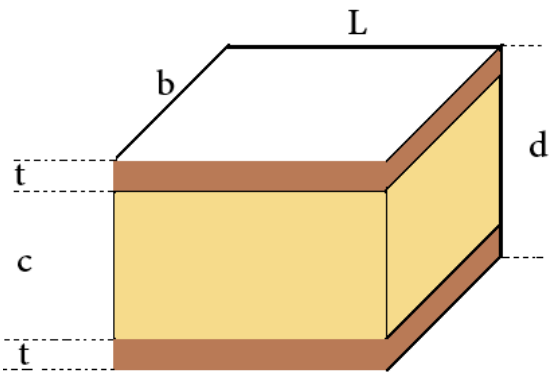

Figure 46: Parameters of a sandwich structure

The material properties usually vary from the standard properties due to different processes of manufacturing; the elastic modulus and shear modulus of the core material can be calculated by following equations:

$$G_c^* = C_2 E_s (\frac{\rho_c^*}{\rho_s})^2 \qquad \textit{Equation 15}$$

G_c^*	Shear modulus of the core.
ρ_c^*	Density of the core.
E_s	Elastic modulus of the bulk core material.
ρ_s	Density of the bulk core material.

The subscript s indicates the standard property of bulk foam material and subscript c indicates the actual material that is being tested here. In this case, it has been assumed that the ρ_c^* is equal to ρ_s and E_s is equal to E_c. The constant C_1=1 and $C_2 = 0.4$.

Then the equivalent bending stiffness EI_{eq} can be calculated by:

$$EI_{eq} = \frac{E_f b t^3}{6} + \frac{E_c b c^3}{12} + \frac{E_f b t d^2}{2} \qquad \textit{Equation 16}$$

For a sandwich structure, the core thickness is much larger than the skin thickness, which means the third term dominates the equivalent bending stiffness and c≅d, therefore, the equation is reduced to:

$$EI_{eq} = \frac{E_f b t c^2}{6} \qquad \textit{Equation 17}$$

The formula of equivalent shear stiffness AG_{eq} is:

$$AG_{eq} = \frac{{G_c}^* b d^2}{c} \approx b c {G_c}^* \qquad \textit{Equation 18}$$

When subject to a load P, the deflection combines both bending deflection and shear deflection.

$$\delta = \delta_b + \delta_s = \frac{PL^3}{B_1 EI_{eq}} + \frac{PL}{B_2 AG_{eq}} \qquad \textit{Equation 19}$$

The values of constant B_1 and B_2 depend on the type of load, which refers to Figure 47 below:

Figure 47: Constant for bending and failure of beams. [3]

By substituting the equations of EI_{eq} and AG_{eq} into the deflection equation and rearranging, the equation can be written in following form:

$$\frac{t}{L} = \frac{2B_2}{B_1} \cdot \frac{{G_c}^*}{E_f(\frac{c}{L})} \cdot \frac{1}{B_2(\frac{\delta}{P}) b {G_c}^* \left(\frac{c}{L}\right) - 1} \qquad \textit{Equation 20}$$

This equation indicates that $\frac{t}{L}$ is a function of $\frac{c}{L}$, each core thickness will correspond to a skin thickness in order to satisfy the constraints on maximum deflection. The optimum combination of core thickness and skin thickness is determined by substituting different values of core thickness into the equation and compare the total weight. This process has been approached by building spreadsheet through Excel, which can be seen in Appendix E.

The equation for stress analysis is listed below:

$$\sigma = \frac{Mc}{I} \qquad \textit{Equation 21}$$

σ	Bending stress at the position (psi)
M	Bending moment at the position (lbf.in)
c	The distance from neutral axis (in)
I	Second moment of inertia of the beam (in^4)

The detailed stress analysis of the redesigned walkway panel will be illustrated in section 6.2.4.

6.2 Replacement of the Walkway Panel

The current walkway panel is made of aluminum and has a weight of 20lbs, the solution of reducing the weight of walkway is to replace the walkway panel by a composite sandwich beam, the supporting beam underneath and two L-beams are not changed. The overall configuration of the walkway in Figure 48: Configuration of walkway panel replacement.

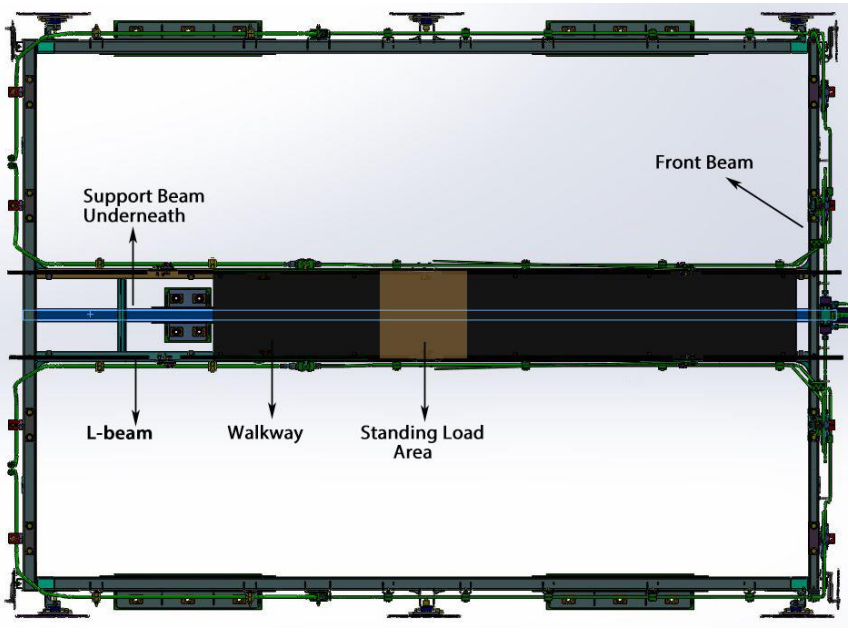

Figure 48: Configuration of walkway panel replacement

In this case, the walkway is supported by two longitudinal L-beam and which is connected to the support beam underneath. A standing load of 300lbs over a 14in*14in area in the middle of the walkway is applied (The Brown square area in the Figure 48). The sanding load is assumed to be a

uniform distributed load. The design is restricted by maximum deflection, which is equal to $\frac{1}{16}$in (0.0625in).

6.2.1 Sandwich Material Selection

To select the optimum material combination, the core thickness from 0.01in to 3.35in has been tested using *Equation 20*, the relationship between total thickness and weight of each material combination has been plotted in Figure 49.

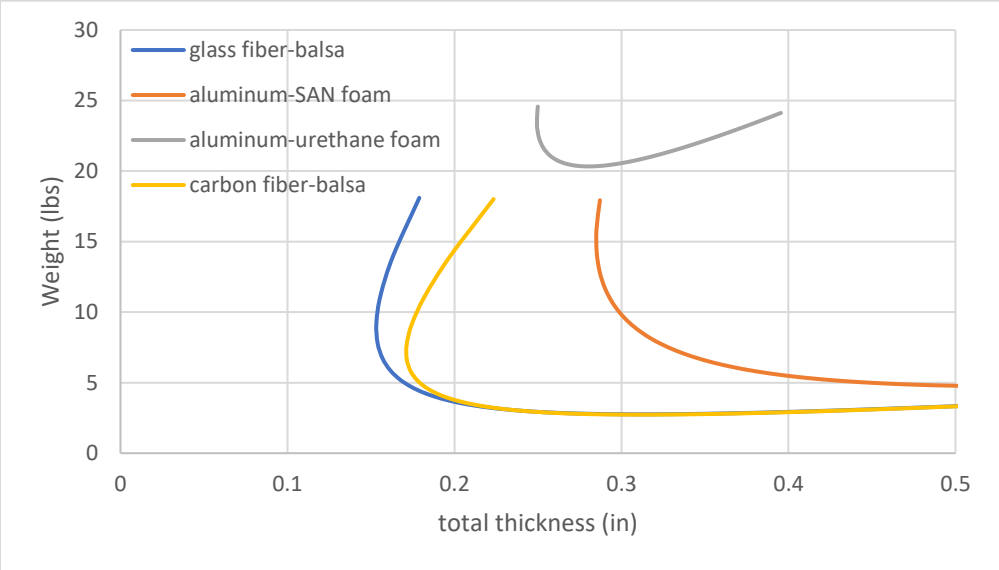

Figure 49: Comparison of different material combinations for panel replacement

The trend of the curve is determined by the relationship between core thickness and skin thickness. The total thickness consists of two skin thicknesses and a core thickness. The skin thickness decreases if core thickness increases in such way that the overall strength of the beam is maintained. Therefore, even at the same thickness, the weight could be different which depends on whether skin or core is dominant. As the total thickness increases exceed a certain value (for example, 0.22in for glass fiber-balsa), the core thickness dominate and each value of total thickness will correspond to a single value of the weight.

The weight of the current walkway panel is 20lbs, and Figure 49 indicates that the combination of aluminum and urethane foam cannot achieve a weight less than 20lbs with guaranteeing the maximum deflection of $\frac{1}{16}$in, so that this material combination has been eliminated. The combination of aluminum and SAN (Styrene acrylonitrile) foam has a larger thickness at the same weight when

comparing to the other two material combinations, therefore, the final decision is to make between carbon fiber-balsa and glass fiber-balsa.

As it has been mentioned before, the carbon fiber could arise galvanic corrosion when get contact with metals, so that the glass fiber – balsa – glass fiber sandwich beam is decided to be the final selection.

6.2.2 Selection of the Dimension of Each Laminate

Firstly, the skin thickness is to be determined. For glass fiber – balsa – glass fiber sandwich beam, the relationship between the total weight and the skin thickness shown in Figure 50.

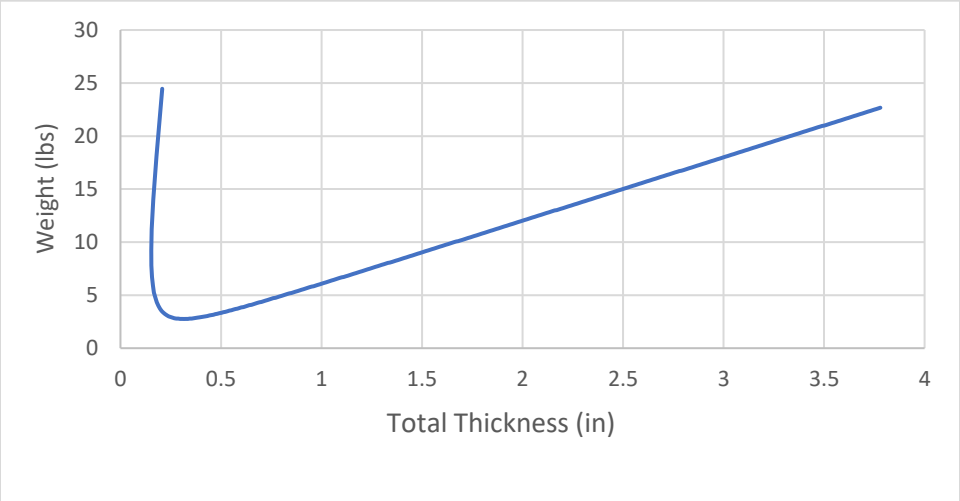

Figure 50. Total thickness of the walkway panel and corresponding total weight

It can be concluded that the minimum weight is 2.8lbs where the skin thickness is 0.0026in. However, it is not feasible to manufacture a glass fiber plate with a thickness of 0.0026in. By doing research on the glass fiber manufacturers, the minimum thickness of the glass fiber fabric is 0.03in and the following technical data sheet of 20 oz woven fiberglass fabric has been found as shown in TABLE XVIII.

TABLE XVIII: DATA SHEET OF FIBERGLASS FABRIC FROM ACP COMPOSITE [4]

Manufacturer	ACP Composite
Fiber type	E-Glass
Density	0.096 lb/in^3
Tensile Strength	500ksi
Tensile Modulus	10.5msi
Thickness	0.03''
Style Number	7587

So that, the skin is decided to be 0.03in thick of woven fiberglass fabric from ACP composite, refer to Appendix E, the corresponding core thickness is 0.1in, where the balsa core is made of Baltek SB.50 [4]. The mechanical properties of the balsa core are shown in TABLE XIX.

TABLE XIX: DATA SHEET OF BALSA CORE FROM BALTEK [4]

		Unit	Baltek SB.50
Standard Sheet	Width	in$\pm\frac{3}{16}$	24
	Length	in$\pm\frac{3}{8}$	48
	Thickness	in +0.01 -0.03	$\frac{3}{16}$ to 3

The minimum thickness of the balsa core is $\frac{3}{16}$in which is equal to 0.1875in, which exceed the designed value of 0.1in, however, the feasibility of manufacturing needs to be considered for the future implementation, therefore, the balsa core thickness is decided to be 0.1875in. The dimensions of each laminate and the weight of the overall sandwich beam are shown in TABLE XX.

TABLE XX: THE FINAL DESIGN OF THE WALKWAY PANEL REPLACEMENT

Parameter	Value
Skin thickness (in)	0.03
Core thickness (in)	0.1875
Total thickness (in)	0.2475
Weight (lbs)	10.9
Old design weight (lbs)	20
Weight reduction (lbs)	9.1

6.2.3 Failure Mode Analysis of the Walkway

There are three failure modes for the walkway: face yielding, face wrinkling and core shear. The configurations and failure load equations of each failure mode are gathered in TABLE XXI.

TABLE XXI: FAILURE MODES OF SANDWICH BEAM [3].

Failure Mode	Configuration	Failure Load
Face yielding	[redacted]	$P \geq \frac{B_3 btc}{l}\sigma_{yf}$
Face wrinkling		$P \geq \frac{B_3 btc}{l} 0.57 (E_f E_s (\frac{\rho_c^*}{\rho_s})^4)^{\frac{1}{3}}$
Core shear		$P \geq C B_4 bc (\frac{\rho_c^*}{\rho_s})^{\frac{3}{2}} \sigma_{ys}$

In these formulas, the constant B is from Figure 47 and the constant C is equal to 0.15. The rest of the variables are the properties of the core/skin material.

By substituting all values in to the failure load equations, the failure load that corresponds to each failure mode is calculated. The results are shown in TABLE XXII.

TABLE XXII: FAILURE LOADS OF THE WALKWAY

Failure Mode	Failure Load
Face yielding	78975 lbf
Face wrinkling	220965 lbf
Core shear	9284 lbf

It can be concluded that the maximum load that the walkway is able to support is 9284lbf without causing failure. However, this value only considers the failure of the walkway, and in this project, the standing load applied to the walkway is 300lbf, which will not cause a walkway failure.

6.2.4 Stress Analysis

The free body diagram of the walkway is as shown in Figure 51.

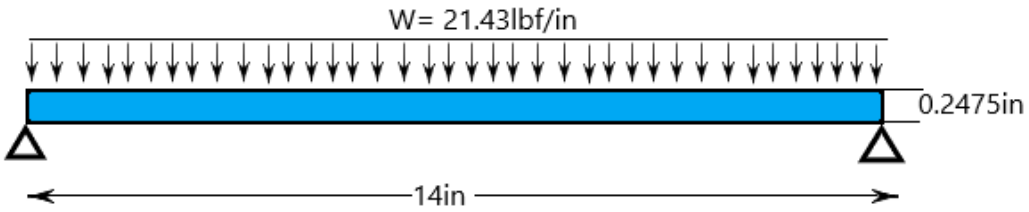

Figure 51: Free body diagram of the walkway

The standing load of 300lbf is assumed to be a pad load within an area of 14in * 14in. Which is equal to the width of the walkway panel, therefore, it has been taken as a uniform distributed load to analyze the stress over the panel. Both ends of the beam are assumed to be fixed (no deflection at both ends). Because the geometry of the beam and applied load are both symmetrical, stress analysis has been performed on a half of the beam. The shear force diagram and bending moment diagram are drawn in Figure 52.

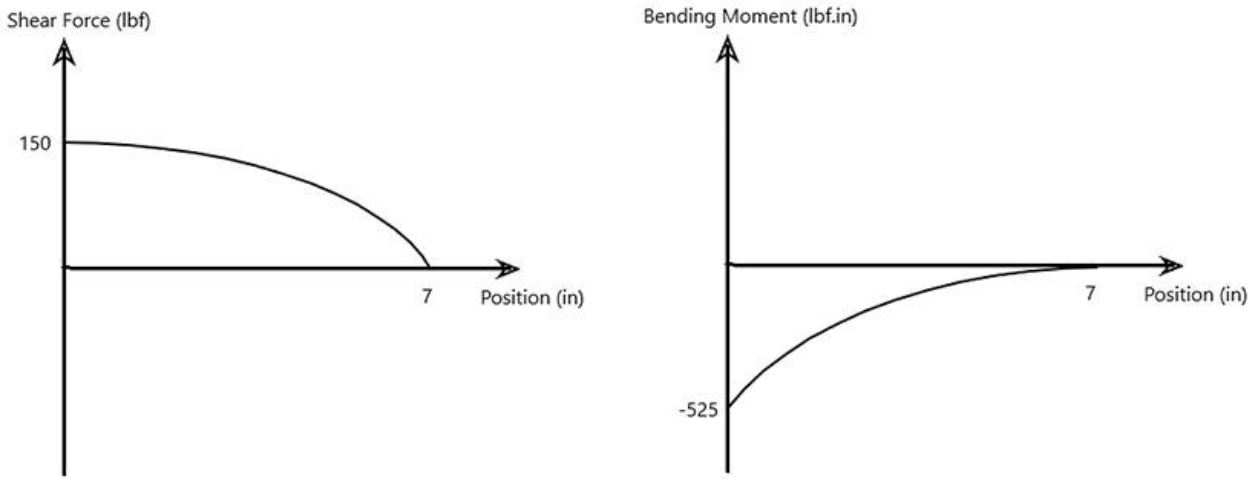

Figure 52: Shear force and bending moment distribution of half of the walkway

The maximum bending moment is at both end of the beam, which is calculated to be equal to 525 lbf-in. By substituting the bending moment into *Equation 21*, the local bending stress at both ends is calculated to be 3673psi.

Similarly, substitute the dimensions of the walkway panel into *Equation 19*, the maximum deflection can be calculated, which is equal to 0.015in. The maximum deflection of the redesigned walkway is less than the allowable maximum deflection of 0.0625in.

6.2.5 FEA Validation

To validate the suitability of the proposed walkway layup components and thicknesses, Bus Riders Consulting performed an FEA study in Ansys. To simplify the analysis, the pad load of 1422 N was applied to a 14x14 in pad at the center of the walkway model, and the sides of the walkway were fixed. These boundary and load conditions can be seen in Figure 53.

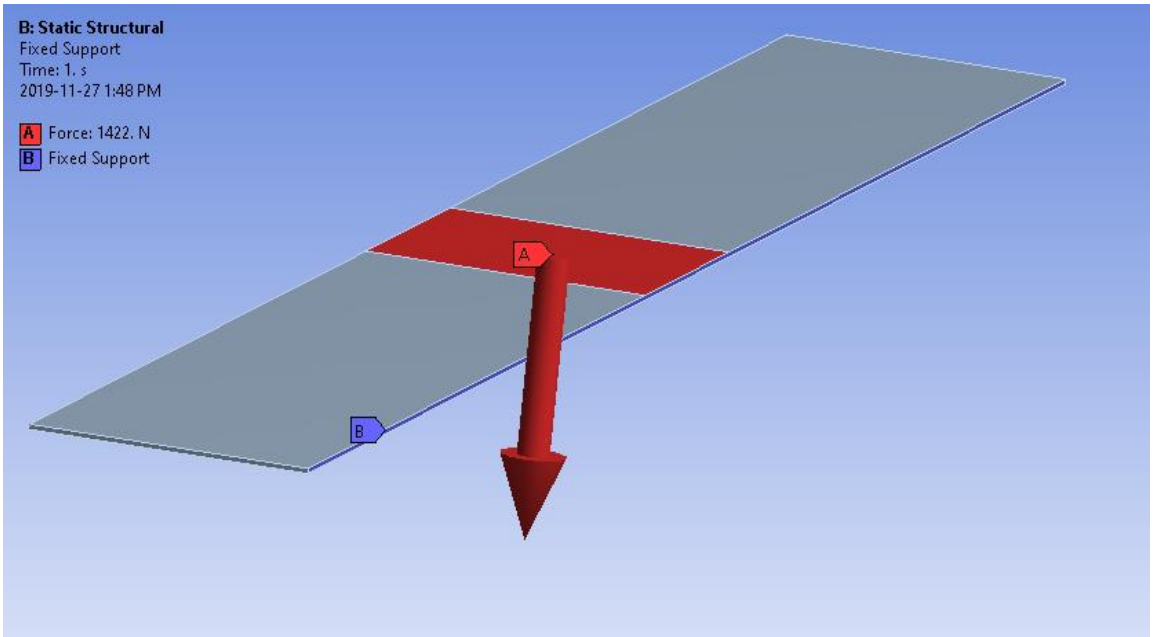

Figure 53: Walkway FEA conditions

Convergence was achieved by performing iterative analysis with increasingly fine meshes and taking the maximum stress at each of the three layers as well as the total maximum deformation each iteration. The values are graphed against the number of nodes, and this process occurs until each value converges. These graphs can be seen in Appendix B

The maximum stress in the GFRP, the balsa, and the maximum walkway deflection can be seen in Figure 54, Figure 55, and Figure 56 respectively.

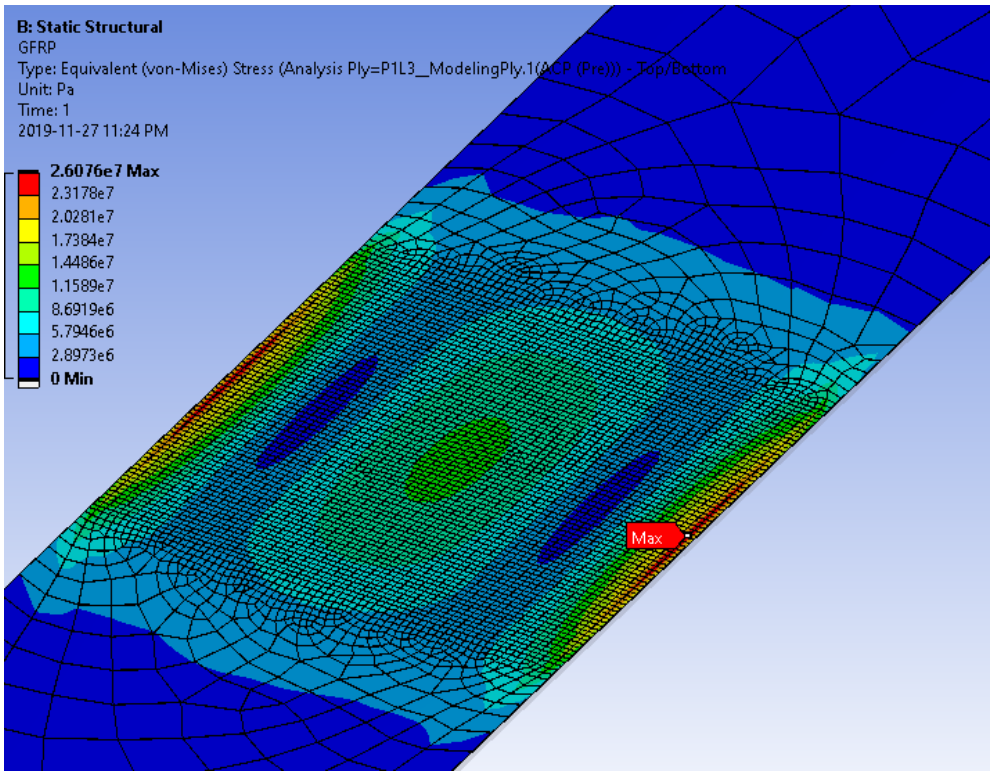

Figure 54: GFRP stress distribution

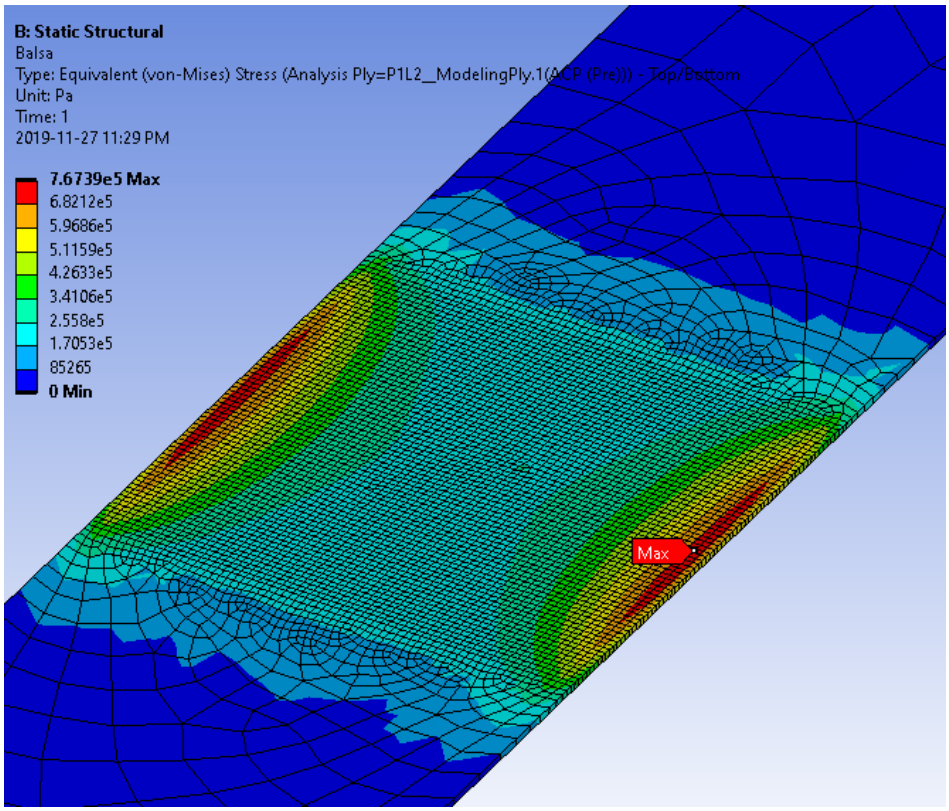

Figure 55: Balsa core stress distribution

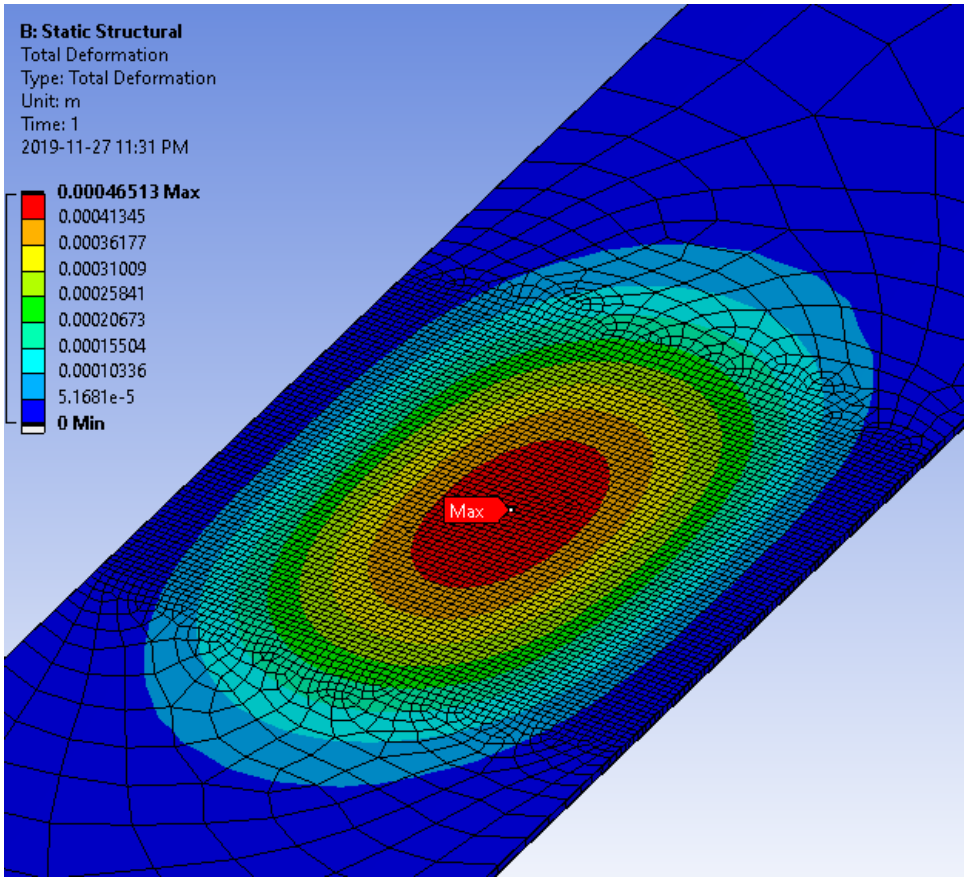

Figure 56: Walkway max deflection

A summary of results from the analysis is shown in TABLE XXIII.

TABLE XXIII: WALKWAY FEA RESULTS

GFRP Max Stress (mPa)	Balsa Max Stress (kPa)	Max Deflection (mm)
26	767	0.46

The maximum stress of the GFRP has been calculated to be 3673psi (25.32MPa), and the maximum deflection of the walkway panel has been calculated to be 0.015in (0.0381mm), therefore, the comparison between FEA results and hand calculation results is shown in TABLE XXIV.

TABLE XXIV: RESULTS COMPARISON

	Results from Hand Calculation	Results from FEA	Percentage Difference (%)
GFRP Maximum Stress (psi)	3673	3770	2.6
Maximum deflection (in)	0.015	0.018	16.7

The percentage difference between calculated maximum deflection and FEA result is 16.7%, and both results are less than the requirement of 0.0625in, so that the redesigned walkway panel is feasible. The maximum stress of 26 MPa (~3770 MPa) is within the 30% yield of the beam to be sourced from ACP Composites which has a maximum allowable stress of 500 ksi (3.4GPa). This satisfies our goal of having the stress within 30% yield.

6.3 Walkway Joints

In order to bolt through sandwich beam, drilling is the only option to make a bolt hole. The mechanism of drilling of composite reinforced parts is different from that of isotropic and homogeneous materials. During drilling of composites, hole propagates at different rates in the various layers. Among them, the most significant factor in balsa are fiber pull-out, fiber breakage matrix cracking and delamination. Drilling is essential for the edge connection in our design since glass fiber sandwich material cannot be welded with aluminum beam. Furthermore, drilling would introduce deformation in the sandwich structure. Therefore, the hole will be drilled oversize and an insert will be epoxied into the hole to increase joint strength. The hole drilled in the walkway will be 1.25" in diameter. A 1.25" High Density Plastic puck with a M6 sized hole will be manufactured internally by New Flyer and inserted to each of the holes for mounting. This can be seen in Figure 57.

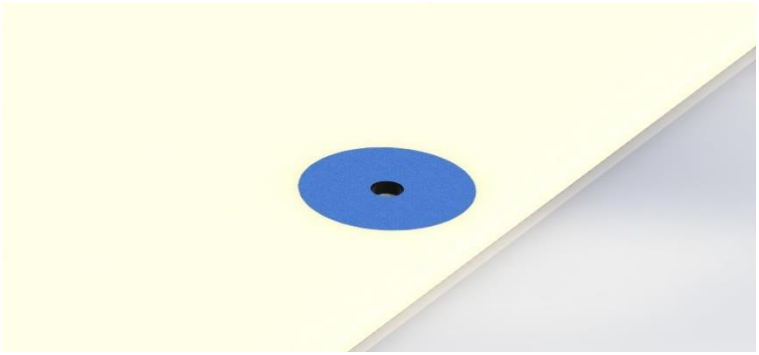

Figure 57: Walkway with joint strengthening puck

The holes on the walkway panel will arise stress concentration which will increase the stress around that area, the maximum stress around the hole can be calculated through:

$$\sigma_{max} = K_t \sigma_0$$

In this equation, K_t is the stress concentration factor for normal stress and σ_0 is the nominal stress in the beam. K_t can be found from using Figure 58.

Figure 58: Stress concentration factor [5]

The outer diameter of the hole is 1.25in, the ratio of $\frac{d}{w}$ is equal to 0.09 and the corresponding value of stress concentration factor K_t is equal to 2.7. Referring to TABLE XXIII, the maximum stress of GFRP and balsa due to stress concentration are calculated to be 70.2MPa and 2.1MPa correspondingly. The tensile strength of the fiberglass is 3447MPa [6] and the tensile strength of the balsa core is 9MPa [4]. Therefore, the clip holes will not arise fractures to the structure.

7 Assembly Overview

Each CNG rack will be assembled with a variety of both mechanical fasteners and adhesives. This section will detail these methods as well as the process to assemble a CNG rack assembly. Each component will be assembled individually before being interfaced together and placed onto the roof of the bus.

7.1 Bolts and Additional Hardware

All hardware used in the assembly of the CNG will follow New Flyer internal specifications. These specifications detail bolt dimensions, material, and are all commonly used in New Flyer assemblies.

7.2 Side Beam

The side beams are where the roof mounts are located, as well as an array of mounts for steel tubing to transfer the CNG for fuel use. In the original rack, both of these components were welded to the side beam, however welding is not a feasible option for jointing steel to fibreglass, so alternative methods must be used.

The primary jointing method for the side beams will be bolts. To further increase the strength of the connections, 3M™ Scotch-Weld™ DP 420 will be used in all steel/aluminum to fiberglass joints due to its high strength, suitability for dissimilar materials, and 20-minute work life [7]. Both the CNG rack roof mounts and the corner nodes must be jointed to the side beams, so enough bolt holes for both of these features must be placed into the beam. The arrangement and dimensions (in inches) of bolt holes in the side beam can be seen in Figure 59.

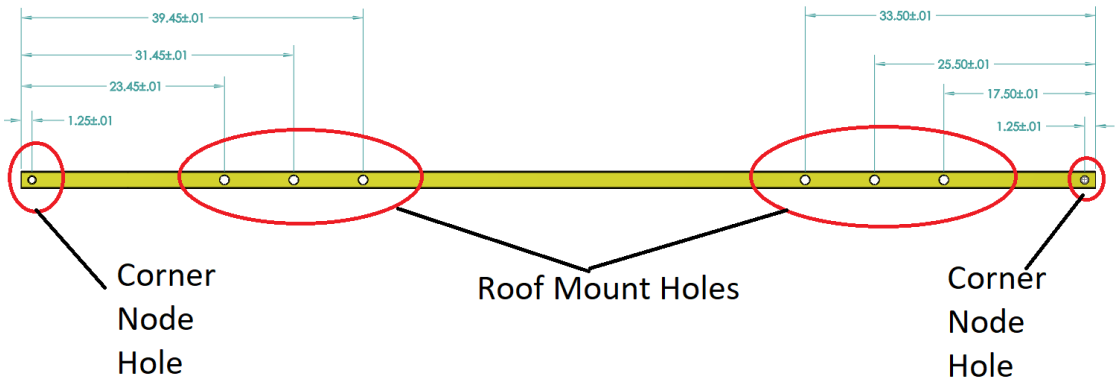

Figure 59: Side beam hole arrangement

Due to fiberglass being a fibrous material, the drilling of holes may decrease strength of the beam, and thus, Bus Riders Consulting determined that adding spacers inside the beam at the bolt connections would provide additional crush resistance and increase clamping force. The side beam will be given a countersunk hole at each roof mount bolt location, with the countersink ending ⅛" from the inner face of the side beam. The spacers will be placed in this slot, and the countersink space will be filled with DP420 epoxy to joint the spacer to the beam and seal the connection. A cross section of the "countersink-spacer" method can be seen in Figure 60.

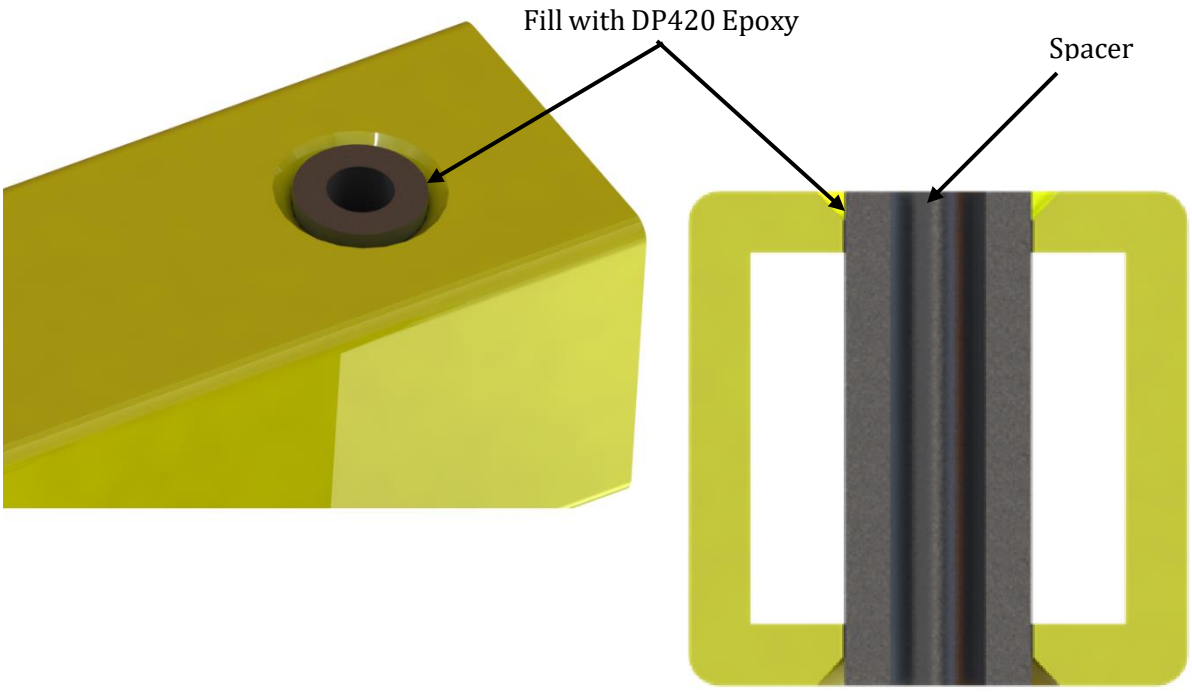

Figure 60: Countersink-spacer method

The roof mounts are sheet metal parts which are folded and welded together, then interfaced to the side beam. They feature slots for weld nuts which are used to bolt the CNG rack to the roof of the bus and are welded to both faces of the side beam along the neutral axis to effectively transfer load. The roof mounts were altered to allow for three ½" diameter, 3.5" length Carbon Steel Grade 8 bolts to be used to joint the mounts to the side beam. The changes to the roof mount can be seen in Figure 61.

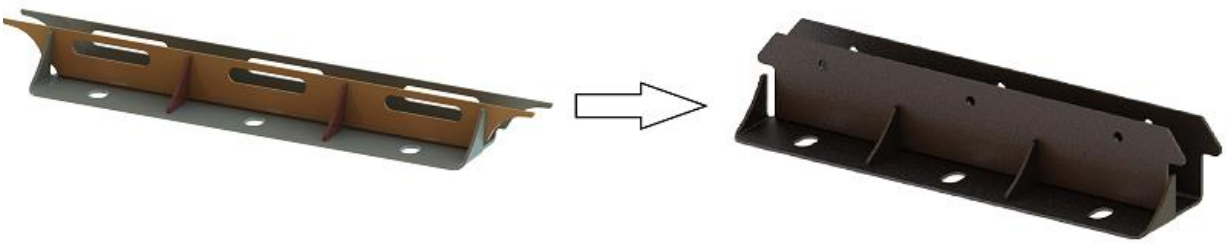

Figure 61: Side beam roof mount changes

Additionally, DP420 will be added between the faces of the side beam and roof mount to increase shear strength of the joint. The selected spacer for the roof mount connection is an aluminum 1” outer diameter unthreaded spacer from McMaster-Carr [8] A cross section of the beam and spacer can be seen in Figure 62.

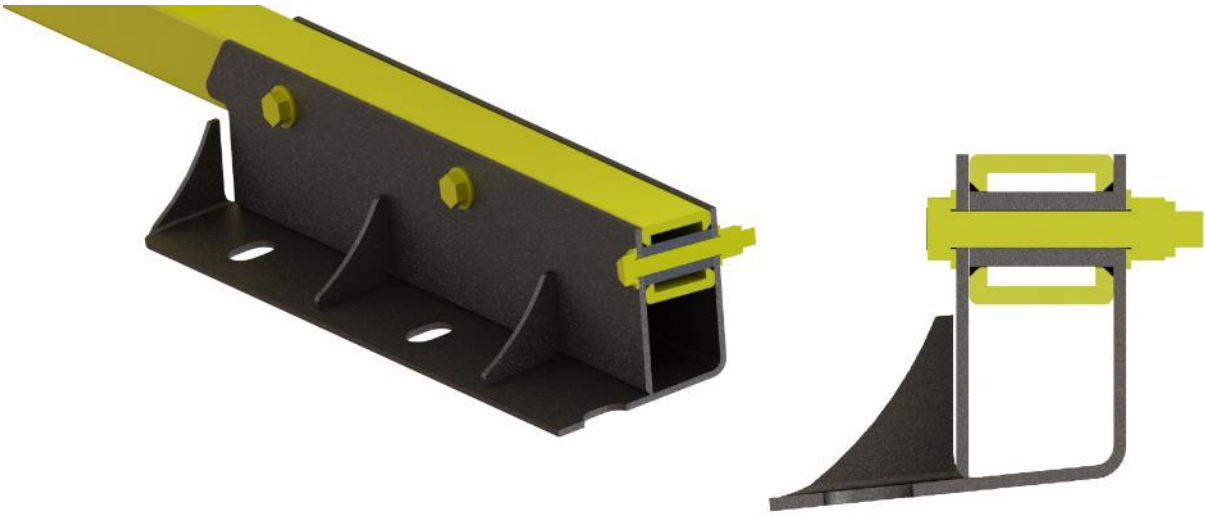

Figure 62: Roof mount side beam joint

The corner nodes will be jointed permanently on both sides of the side beam. A single ⅜” bolt hole with a ¾” outer diameter spacer also sourced from McMaster-Carr [9] will be used as the bolt interface at these locations. Additional DP420 will be put between the corner node and side beam to further increase joint strength and make the interface permanent. Bosses on the corner node inner faces will allow a glue gap between the corner node and side beams to exist. A cross section of the joint can be seen in Figure 63.

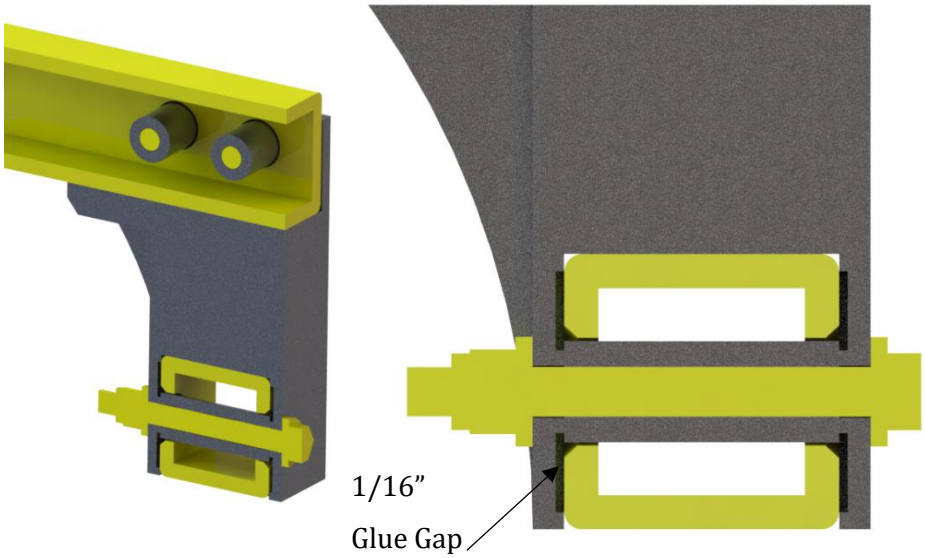

Figure 63: Corner node joint

The mounts for the tubing will simply be mounted to the side beam using DP420. Two of these side beam assemblies are required per CNG rack assembly. The handedness of the assembly is not critical, so two identical side beams can be made. An overview of the side beam assembly can be seen in Figure 64.

Figure 64: Side beam assembly

7.3 Front Beam

The front beam features four separate joint styles: The corner node, the CNG tanks, the L-brackets for the walkway, and the center beam. Much like the side beam, the front beam joints will be comprised of both bolt connections and DP420 epoxy strengthening adhesive. The locations of holes for the front beam can be seen in Figure 65.

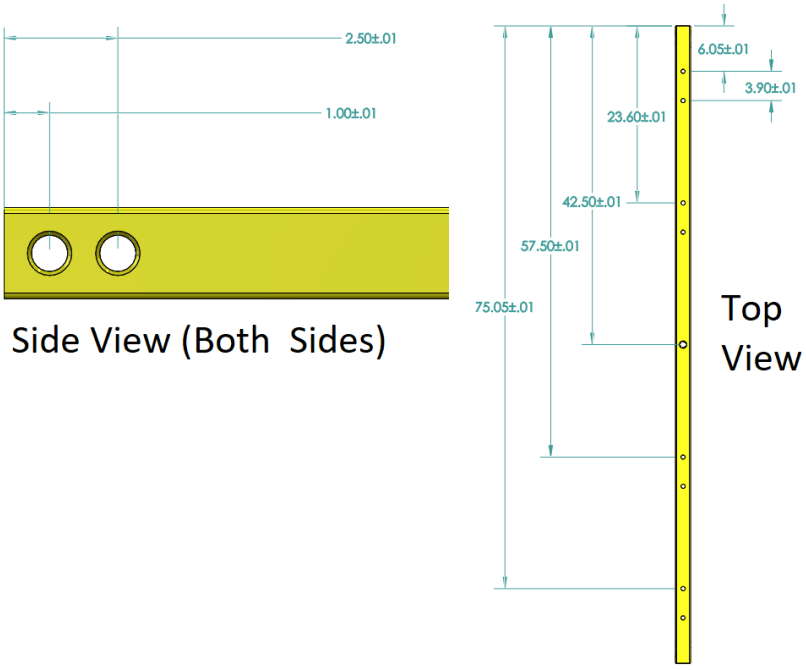

Figure 65: Front beam hole arrangement

The corner node jointing is two ⅜" bolt holes with the ¾" outer diameter spacers. The method of countersinking the hole, adding the spacer, and filling the hole with epoxy will be used for these sections as well. This is required on both sides of the front beam. No DP420 will be used in this joint to allow for removal of the beam if need be. A cross section of this joint can be seen in Figure 66.

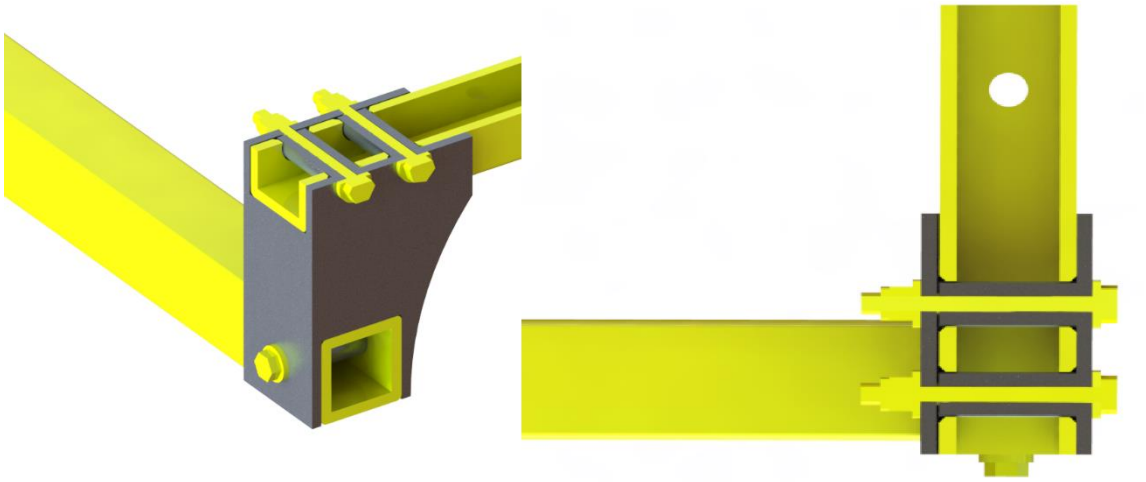

Figure 66: Corner node to front beam joint

The CNG tanks will be mounted in the same manner as the original rack, with two 0.5” diameter, 7” length carbon steel grade 8 bolts being placed in four locations and large diameter clamps securing the CNG tanks. Spacers will be installed in these bolt holes with the aforementioned countersink-epoxy method. The CNG tank holes are made on the front beam, but the tanks are not installed until the very end of the assembly. A cross section of a single CNG tank joint can be seen in Figure 67.

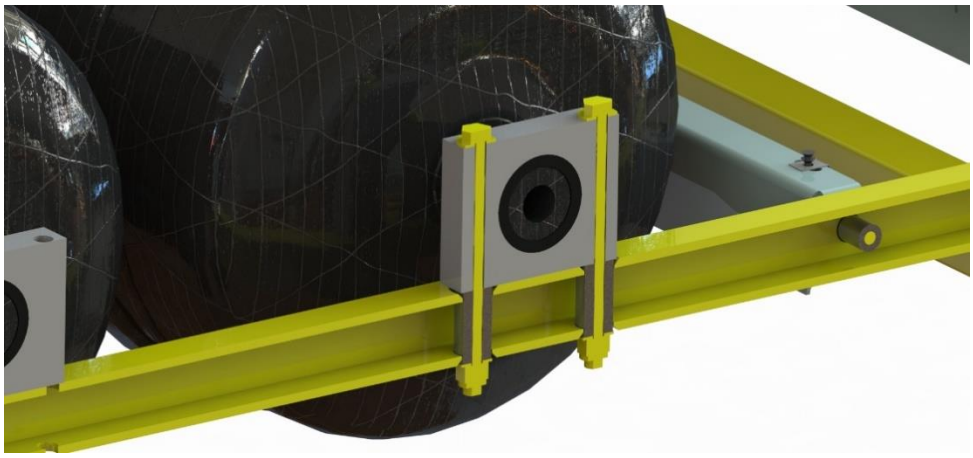

Figure 67: CNG tank joint

The L-brackets which support the walkway were previously welded to the front beam. They are folded sheet metal parts and were modified to allow bolting to the front beam. An additional flange

was added at both ends of the brackets and given a ⅜" diameter hole. DP420 adhesive is used between the L-bracket face. The countersink-epoxy method is used to install the ¾" spacers, of which two are needed per front beam. The L-bracket joint cross section can be seen in Figure 68.

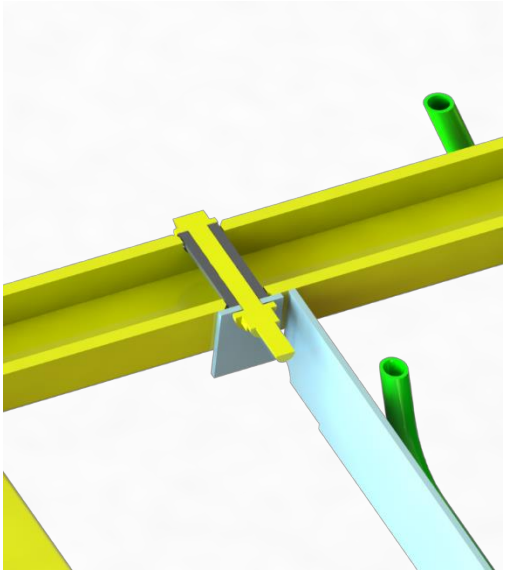

Figure 68: L-bracket to front beam joint

The center beam joint consists of a single countersunk-spacer hole for a 3/8" bolt at the center of the front beam. A 5" bolt is used to joint the two beams together. The joint cross section can be seen in Figure 69.

Figure 69: Center beam to front beam joint

7.4 Center Beam

The center beam also features two roof mount pads, as well as is jointed to the front beam. The holes at the ends of the center beam follow the same countersink-spacer method as the front beam here, and the cross section was shown in Figure 69.

The center beam has a four-inch overhang on the rear end of the rack. This overhang contains a slot at which a bracket is installed which mates the CNG rack assembly to a mirror assembly, as each bus contains two CNG rack assemblies. Each center beam also joints re-designed footpads with two ⅜" bolts. These locations follow the countersink-spacer method. A cross section of the center beam-roof mount joints can be seen in Figure 70.

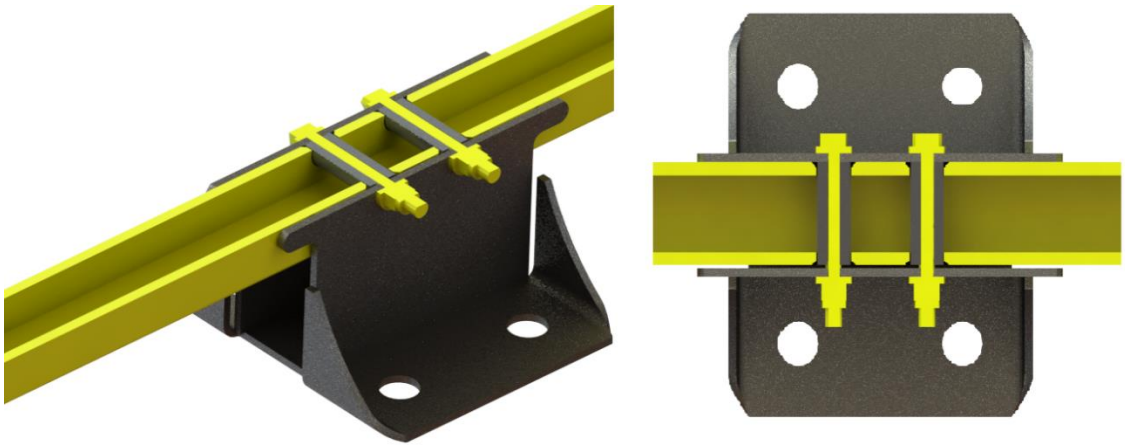

Figure 70: Center roof mount joint

An overview of the assembly at this point can be seen in Figure 71

Figure 71: CNG rack without walkway

7.5 Walkway

The current walkway panel is fixed on the two L-beams through the use of M6 U-nuts from Tinnerman [10] as well as a panhead M6 carbon steel screw. The supporting L-beams geometry at these areas are not changing, so the same method will be used to mount the re-designed walkway panel. Each L-bracket contains nine U-nuts and requires nine screws for the walkway. A single walkway joint can be seen in Figure 72 (The interface between the U-nut and L-bracket is due to the fact that the U-nut is spring steel and clips on the bracket).

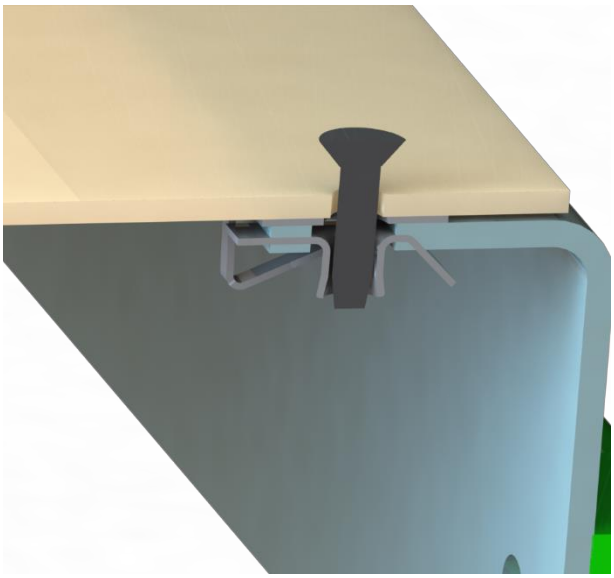

Figure 72: Walkway joint

7.6 Assembly Order

The previous sections detail the information of each joint used, but not necessarily the order of operations for manufacturing. The assembly plan does not detail manufacturing of individual components, nor the steps to manufacturing assemblies that were not altered on the CNG rack. The steps to assemble a CNG rack in the context of each part as well as the overall assembly are shown in TABLE XXV.

TABLE XXV: ASSEMBLY ORDER

Step #	Part Worked on	Items Required	Qty	Description
1	Side Beam	Side Beam	2	Create hole pattern with countersink holes for spacers
		Drill Size 3/4"	1	
		Drill Size 1"	1	
		Countersink Mill	1	
2	Side Beam	Side Beam with holes	2	Install spacers into countersunk holes, fill countersink with epoxy
		92510A814 Spacer	4	
		925102A832 Spacer	12	
		3M DP420 Epoxy	N/A	
3	Side Beam	Side Beam with spacers	2	Install footpads to side beam with hardware, coat mating faces with DP420
		Roof Mount Pads	4	
		1/2" hardware (bolt, nut, washer)	12	
		3M DP420 Epoxy	N/A	
4	Full Assembly	Side Beam	2	Install corner nodes to side beams with hardware, full corner node glue gap with epoxy
		Corner Node	4	
		3/8" hardware (bolt, nut, washer)	4	
		3M DP420 Epoxy	N/A	
5	Front Beam	Front Beam	2	Create hole pattern with countersink holes for spacers
		Drill Size 3/4"	1	
		Drill Size 1"	1	
		Countersink Mill	1	
6	Front Beam	Front Beam with holes	2	Install spacers into countersunk holes, fill countersink with epoxy
		92510A814 Spacer	14	
		925102A832 Spacer	16	
		3M DP420 Epoxy	N/A	
7	Full Assembly	Side Beams with corner nodes	2	Mount front beams onto corner nodes
		Front beams with spacers	2	
		3/8" hardware (bolt, nut, washer)	8	
8	Center Beam	Center beam	1	Create hole pattern with countersink holes for spacers
		Drill Size 3/4"	1	
		Drill Size 1"	1	
		Countersink Mill	1	

Step #	Part Worked on	Items Required	Qty	Description
9	Center Beam	Center beam with holes	1	Install spacers into countersunk holes, fill countersink with epoxy
		92510A814 Spacer	2	
		925102A832 Spacer	4	
		3M DP420 Epoxy	N/A	
10	Center Beam	Center beam with spacers	1	Install footpads to center beam with hardware, coat mating faces with DP420
		Center footpads	2	
		1/2" hardware (bolt, nut, washer)	4	
		3M DP420 Epoxy	N/A	
11	Full Assembly	Center beam with footpads	1	Mount center beam onto assembly
		Full assembly	1	
		3/8" hardware (bolt, nut, washer)	2	
12	Full Assembly	Full assembly	1	Mount L-brackets onto full assembly
		L brackets	2	
		3/8" hardware (bolt, nut, washer)	4	
13	Full Assembly	Walkway	1	Mount walkway onto assembly with u-nuts and screws
		Full assembly	1	
		U-Nuts	18	
		M6 screw	18	
14	Full Assembly	CNG Tank	4	Mount CNG Tanks onto full assembly
		Clamps	8	
		1/2" hardware (bolt, nut, washer)	16	

The mounts existing for the tubing on the rack are added intermittently throughout this process by using DP420 to joint the steel to beams.

7.7 Failure Mode and Effect Analysis

The Failure Mode and Effects Analysis (FMEA) has been performed to the final assembly of the redesigned CNG rack, which is only constrained on the parts that has been redesigned: the front beams, the side beams, the corner nodes as well as the walkway panel. The results of failure modes analysis are shown in Figure 73.

Item	Failure Mode	Failure Effects	SEVERITY (S)	Potential Causes	OCCURRENCE (O)	Current Controls	DETECTION (D)	RPN	Action Recommended	SEVERITY (S)	OCCURRENCE (O)	DETECTION (D)	RPN
Walkway Panel	Water seep into the balsa core	The total weight is increased and mechanical strength is weakened	5	The water could seep into the inside of the beam through the screw holes.	6	inspection	7	210	Add a washer to the screw holes.	5	2	7	70
Walkway Panel	Corrosion joint screws	Losing strength, cause failure of the joints.	6	The screw holes are holding moistures.	6	inspection	3	108	Add a washer to the screw holes.	6	2	3	36
Walkway Panel	Fiber glass material weakened	The walkway will get brittle and easy to fracture.	9	The UV light from sunlight will waken the fibre strength of the fiberlass.	8	inspection	8	576	Add a UV coating to the walkway panel	9	2	8	144
Walkway Panel	Slippery surface for workers	Workers could be injured	8	The fibreglass surface is smooth and cannot provide enough friction	6	people need to take care of walking on the walkway	6	288	Add a texture coating to the walkway panel	8	2	6	96
Front Beam	Fiber glass material weakened	The fibreglass will get brittle and easy to fracture.	9	The UV light from sunlight will waken the fibre strength of the fiberlass.	7	periodic inspection	8	504	Add a UV coating to the walkway panel	9	1	8	72
Side Beam	Fiber glass material weakened	The fibreglass will get brittle and easy to fracture.	9	The UV light from sunlight will waken the fibre strength of the fiberlass.	7	periodic inspection	8	504	Add a UV coating to the walkway panel	9	1	8	72

Figure 73: Failure mode and effect analysis

The most critical failure mode is the accelerating of material degradation of glass fiber due to the UV radiation, such that the mechanical strength of the glass fiber will be reduced significantly. As the CNG rack is located at the roof, where the structure is exposed to large amount of solar radiation, therefore, this potential failure mode needs to be removed immediately. There is a short-term UV exposure test of E-glass fiber and the results are shown in Figure 74.

Figure 74. Effect of UV exposure to the strength of E-Glass fiber [11]

There are three specimens of E-glass fiber, where EG1, EG2 and EG3 corresponds to 1 layer, 2 layers and 3 layers of E-glass fiber respectively. The maximum UV exposure time is 90 days in this experiment, which is a short-term test.

In the short-term test, the tensile strength of the glass fiber is increased a little firstly and then keeps decreasing, which is because of the forming and destroying of the internal chemical bond energy due to UV exposure [11]. For long-term use, the UV protection is necessary.

Therefore, an UV coating is added to the surface of glass fiber material. A potential selection of the UV coating is 3M™ Automotive Film FX ST Series [12]. The UV coating will be applied to the walkway panels and all glass fiber beams (front beams and side beams).

8 Manufacturing Methods and Sourcing

Several methods will be used in the manufacturing of the components in the re-designed CNG rack. This section will detail those methods and discuss their advantages and why they were selected by Bus Riders Consulting. A bill of martials

8.1 Pultrusion

The pultrusion process is used to manufacture the front, side and center beams. It is continuous process, the reinforcing fiber pulled through heated resin bath and the formed into required shape as it passes through bushings. After that, it moves through a lengthy heated die, where it gets its net shape and cures. Further downstream, after cooling, the resulting profile is cut to desired length. Pultrusion produces smooth finished parts that do not require post-processing. The main advantages of pultrusion are low cost process as compare to other available options and produce custom designed and non-corrosive features of fiberglass reinforced polymer and eco-friendly [13].

Creative Pultrusions [1] is the selected supplier for the beams in the re-designed CNG rack, as they offer off the shelf cross sections of structural pultruded beams of 2x2 outer dimensions with a ¼" wall thickness. Their series 1525 beams in this dimension cost $10.87 CAD per ft and are fire retardant.

8.2 Corner Node Die Casting

Die casting is a manufacturing process which use to produce geometrically complex metal parts by forcing molten metal under high pressure into a mold cavity. Manufacture of parts using die casting is reasonably simple, containing five main steps, which are Clamping, Injection, Cooling, Ejection, and Trimming. The metal such as nonferrous alloy is melted in the furnace and then injected into the mold cavity in the die casting machine. There are two different type of die casting machine- hot and cold used for metal casting depending upon the nature of metal. The cold chamber machine used for alloys with high melting temperature and the hot chamber machine used for alloys with low melting temperature. However, after the molten process the metal is injected into the dies then instantly cooldown and solidifies into the final part and this complete process is called the die casting. The main advantage of die casting is it can produce large parts and form many complex geometries with good surface finish and high accuracy. The production rate is very high and reduces labour cost with high tooling [14].

Titan Foundries is a local Winnipeg foundry with a working relationship with New Flyer, and they are they selected supplier for the die cast corner nodes. Creation of the corner node die will cost an estimated $2,500-$3,000, and each part will cost ~$100.

8.3 Walkway Manufacturing

The Light Resin Transfer Molding is proposed method to manufacture Glass fiber-balsa-glass fiber sandwich structure. it is a process in which composite products are manufactured by using a closed mold system. The RTM lite process is used where we have tight dimensional tolerance. Sandwich core laminates are defined as a layered material with two thin, stiff and high strength outer faces bonded to a thick and low weight core material. The laminate built in three layers: Skin-core-skin by placing dry fabrics under the pressure of vacuum will cause them to compress. The main advantage of RTM lite are it reduces labour cost, low waste, and high productivity. A potential manufacturer of doing RTM Lite is JHM Technologies Inc [15]. And the proposed laminate schedule for walkway is as shown in Table XXVI.

Table XXVI: PROPOSED LAMINATE SCHEDULE

Ply	Material	Thickness [in]
P1	E-Glass Fiber	0.03
P2	Baltek SB.50	0.1875
P3	E-Glass Fiber	0.03

8.4 Bill of Materials

An estimated cost as well as the supplier for all components required to develop a full CNG rack assembly (I.e. 8 CNG tanks) can be seen in TABLE XXVII.

TABLE XXVII: BILL OF RAW MATERIAL

Item	Specifications	Description	Supplier	Quantity	Unit Cost	Total Cost
Front Beam	85in length	Commercially available 2x2 in GFRP pultruded beams with a 1/4" wall thickness	Creative Pultrusions	4	$ 80.00	$ 320.00
Side Beam	124in length	Commercially available 2x2 in GFRP pultruded beams with a 1/4" wall thickness	Creative Pultrusions	4	$ 115.00	$ 460.00
Center Beam	124	Commercially available 2x2 in GFRP pultruded beams with a 1/4" wall thickness	Creative Pultrusions	2	$ 115.00	$ 230.00
1/2" Spacers	1" OD, 2in length	Unthreaded Aluminum spacers	McMaster Carr	64	$ 10.68	$ 683.52
3/8" Spacers	3/4" OD, 2in length	Unthreaded Aluminum spacers	McMaster Carr	40	$ 4.42	$ 176.80
3M DP420 Epoxy	2 Part 5 Galleon Drum	High strength two-part epoxy	3M	1	$ 300.00	$ 300.00
Corner Node Die	Custom Die for Casting	Custom die for casting of the corner nodes	Titan Foundries	1	$ 3,000.00	$ 3,000.00
Corner Node	Casting of the corner node	Casting of the corner node	Titan Foundries	8	$ 100.00	$ 800.00
E Glass Fiber Sheet	180in length, 38in width, 0.03in thick	Face sheet for the walkway fiber sandwich	ACP Composite	2	$ 82.00	$ 164.00
Baltek Sheet	48in length, 24in width, 0.1875in thick	Core sheet for the walkway fiber sandwich	Baltek Inc.	6	$ 14.40	$ 86.40
Total						$ 6,220.72

9 Conclusion

Bus Riders Consulting has investigated alternative materials to replace the existing heavy and overdesigned components on the Compressed Natural Gas (CNG) support racks. Structural components have been analyzed and new materials have been selected and validated for static loading conditions. The functionality of the rack has been maintained and mounting locations for tubing and roof mounting did not change. The previous CNG rack with attachments can be seen compared to the new CNG rack to prove this in Figure 75.

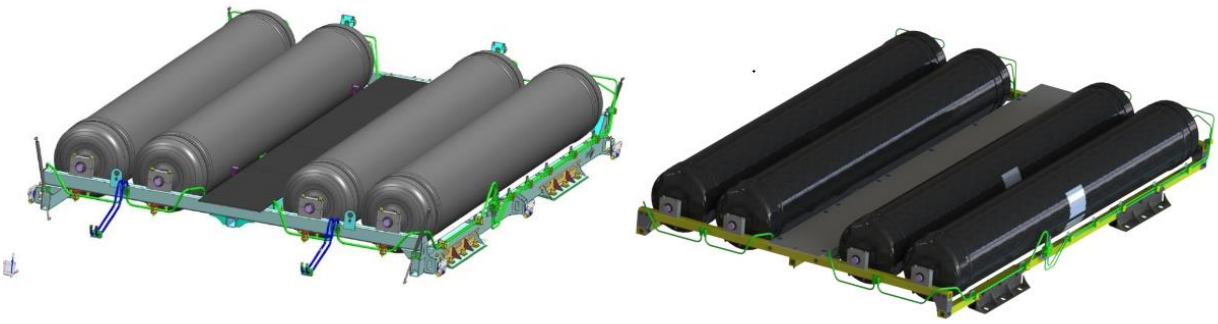

Figure 75: Old CNG rack vs new CNG rack

A summary of the weight comparison between the old CNG rack and new rack is shown in TABLE XXVIII.

TABLE XXVIII: WEIGHT COMPARISON

Old Rack				New Rack			
Component	Weight	Qty	Total	**Component**	Weight	Qty	Total
Front Beam	27.5	2	55	**Front Beam**	14.5	2	29
Side Beam	48.9	2	97.8	**Side Beam**	21	2	42
Center Beam	32.2	1	32.2	**Center Beam**	21.7	1	21.7
Corner Node	2.4	4	9.6	**Corner Node**	2.3	4	9.2
Walkway	28.7	1	28.7	**Walkway**	12.7	1	12.7
				Extra Components	-	-	10
		Total Weight (lbs)	223.3			Total Weight (lbs)	124.6

An extra 10lbs was added to the new rack weight to account for the extra mechanical hardware added for mounting. The final weight comparison can be seen in TABLE XXIX.

TABLE XXIX: FINAL WEIGHT COMPARISON

	Weight (Lbs)
Old Rack	223.3
New Rack	124.6
Savings per rack	98.7
Savings per bus	197.4

A weight savings of nearly 200lbs per bus exceeds our established goal of 150lbs. As such, Bus Riders Consulting successfully completed the task assigned by New Flyer. A prototype can be manufactured using the assembly plan set out prior, and a bill of material stated that the cost of such a prototype would be ~$6,300 CAD.

9.1 Future Considerations

The analyses performed in this project generally only considered equivalent static loading. Vibration analysis on FEA was not feasible in this project to due node restrictions on Ansys, and as such a numerical vibration lifetime study would not have been feasible. Additionally, a prototype could not be built, so no physical testing could be performed. Following the steps to manufacture a prototype, then performing vibration testing would provide further information on the validity of the design.

References

[1] Creative Pulstrusions, "Standard Structural Profiles - Pultruded Square Tube," Creative Pultrusions, [Online]. Available: https://www.creativepultrusions.com/index.cfm/products-solutions/fiberglass-structural-profiles/standard-structural-profiles-pultruded-square-tube/. [Accessed 11 November 2019].

[2] "Creative Pultrusion," [Online]. Available: https://www.creativepultrusions.com/index.cfm/data/product-literature/pultexc2ae-pultrusion-design-manual1/. [Accessed 2019].

[3] "VectorLam 2.0," VECTORPLY, [Online]. Available: http://vectorlamcirrus.cloudapp.net/.

[4] "Strength of Sandwich Structures," [Online]. Available: http://www.mse.mtu.edu/~drjohn/my4150/sandwich/sp2.html.

[5] "BALTEK SB DATA SHEET," 3A CORE MATERIALS, [Online]. Available: https://www.3accorematerials.com/uploads/documents/TDS-BALTEK-SB-E_1106.pdf.

[6] Budynas-Nisbett, Shigley's Mechanical Design 8th Edition, McFraw-Hill.

[7] "Woven Fiberglass," ACP Composite, [Online]. Available: https://crockercommerce.azureedge.net/0012-content/Fiberglass-Fabric-PDS.pdf.

[8] 3M, "3M™ Scotch-Weld™ Epoxy Adhesive DP420," [Online]. Available: https://www.3mcanada.ca/3M/en_CA/company-ca/all-3m-products/~/3M-Scotch-Weld-Epoxy-Adhesive-DP420/?N=5002385+3293242436+3294529206&rt=rud. [Accessed 20 November 2019].

[9] McMaster-Carr, "Aluminum Unthreaded Spacer," [Online]. Available: https://www.mcmaster.com/92510a832. [Accessed 20 November 2019].

[10] McMaster-Carr, "Aluminum Unthreaded Spacer," [Online]. Available: https://www.mcmaster.com/92510a814. [Accessed 21 November 2019].

[11] ARaymond, "2016 Product Catalogue," 2016. [Online]. Available: https://www.araymond-automotive.com/sites/default/files/medias/document/2017/AR-Product-Catalog-Raysource-2016-EN_1.pdf. [Accessed 24 November 2019].

[12] Z. Jun, C. Gaochuang, C. Lu, S. L. Amir and D. T. Konstantinos, "Deterioration of Basic Properties of the Materials in FRP-Strengthening RC Structures under Ultraviolet Exposure," 30 August 2017. [Online]. Available: http://eprints.whiterose.ac.uk/120688/1/polymers-09-00402.pdf.

[13] "Automotive window films," 3M, [Online]. Available: https://www.3mcanada.ca/3M/en_CA/post-factory-installation-ca/automotive-window-films/.

[14] "ALL ABOUT THE PULTRUSION PROCESS," BEDFORD REINFORCED PLASTICS, [Online]. Available: https://bedfordreinforced.com/app/uploads/2017/12/all-about-the-pultrusion-process.pdf.

[15] "About Die Casting," Pace Industries, [Online]. Available: https://paceind.com/die-casting-101/die-casting-faqs/what-is-die-casting/. [Accessed 30 11 2019].

[16] "Light RTM Process (LRTM)," JHM Technologies Inc., [Online]. Available: https://www.rtmcomposites.com/process/light-rtm-lrtm.

Appendix A – Front Beam Hand Calculations

The following calculations are how the reaction forces were obtained for the existing front beam design.

$$F_A + F_B = 358 + 358$$

$$F_A + F_B = 716\ N$$

$$F_B = \frac{(358)(0.203) + (358)(0.203 + 0.446)}{(1.08)}$$

$$F_B = \ 283\ N$$

$$F_A + 283 = 716\ N$$

$$F_A = 433\ N$$

With the reaction forces solved, shear and moment diagrams were plotted which is shown in Figure A- 1

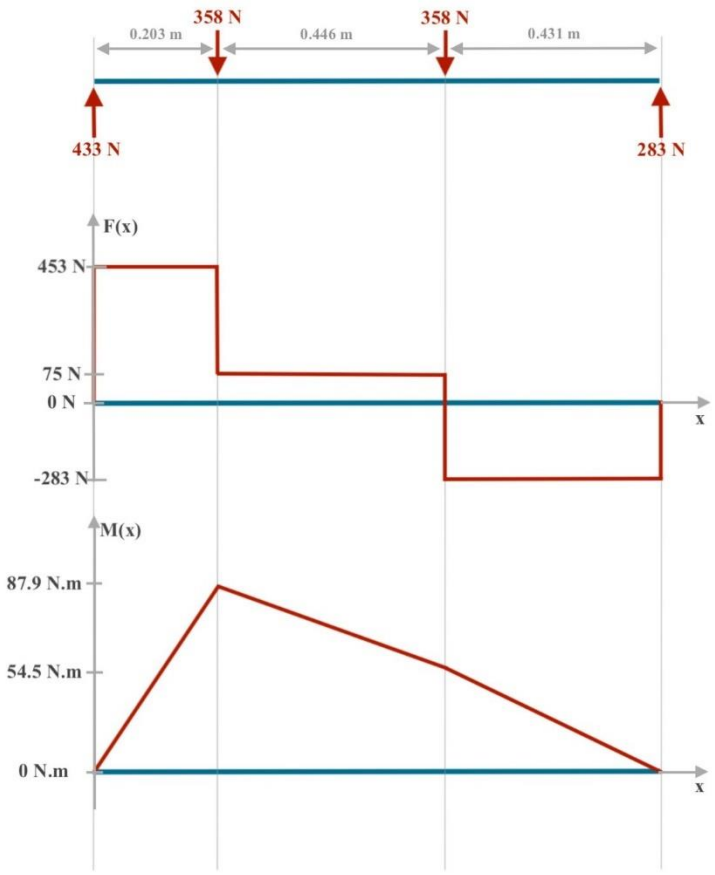

Figure A- 1: Shear and moment diagrams of front beam

Using the highest bending moment value (87.9 N.m) observed from the moment diagram, the following calculation was done to determine the maximum bending stress. Existing beam dimensions are shown in TABLE A- 1.

$$\sigma_{bending} = \frac{(M)(y)}{I}$$

$$I = \frac{(b)(h^3)}{12}$$

TABLE A- 1: EXISTING BEAM DIMENSIONS

Front Beam	1	
Height	3 in	0.0762 m
Width	2 in	0.0508 m
Thickness	0.125 in	0.003175 m

$$I = \frac{(0.0508)(0.0762^3)}{12} - \frac{(0.0445)(0.07015^3)}{12}$$

$$I = 5.93 \times 10^{-7} m^4$$

The I is the moment of inertia based on the cross section of the rectangular tube.

$$\sigma_{bending} = \frac{(87.9)\left(\frac{0.0762}{2}\right)}{5.93 \times 10^{-7}}$$

$$\sigma_{bending} = 5.65\ MPa$$

Appendix B – FEA Convergence Plots

Convergence of FEA result is required to ensure the validity of the simulation. This appendix summarizes all FEA convergence plots for the six cases. The six FEA cases are:

- Front Beam – Figure B-1
- Side Beam - Figure B-2
- Center Beam - Figure B-3
- Corner Node Static - Figure B-4
- Corner Node Braking - Figure B-5
- Walkway – Figure B-6

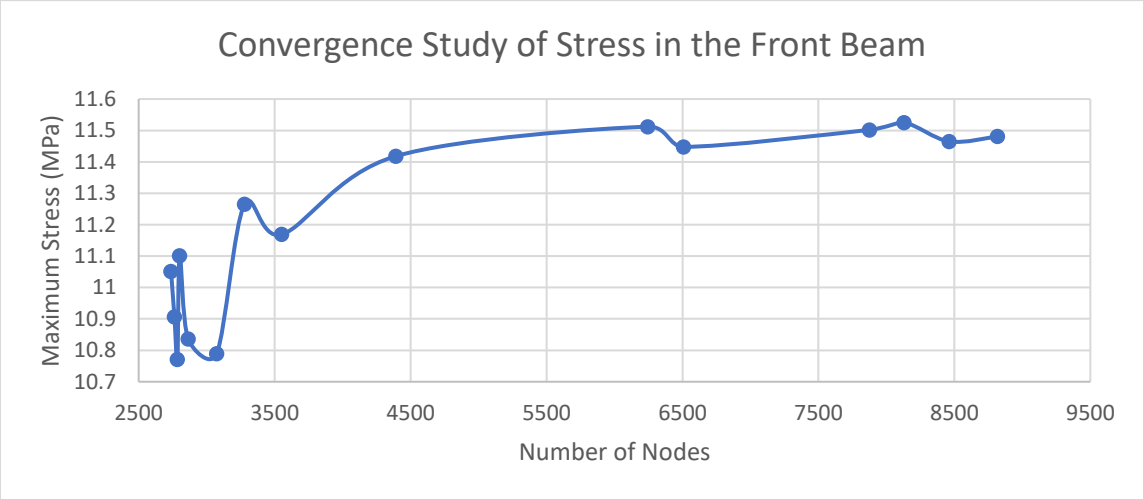

Figure B-1: Front beam convergence plot

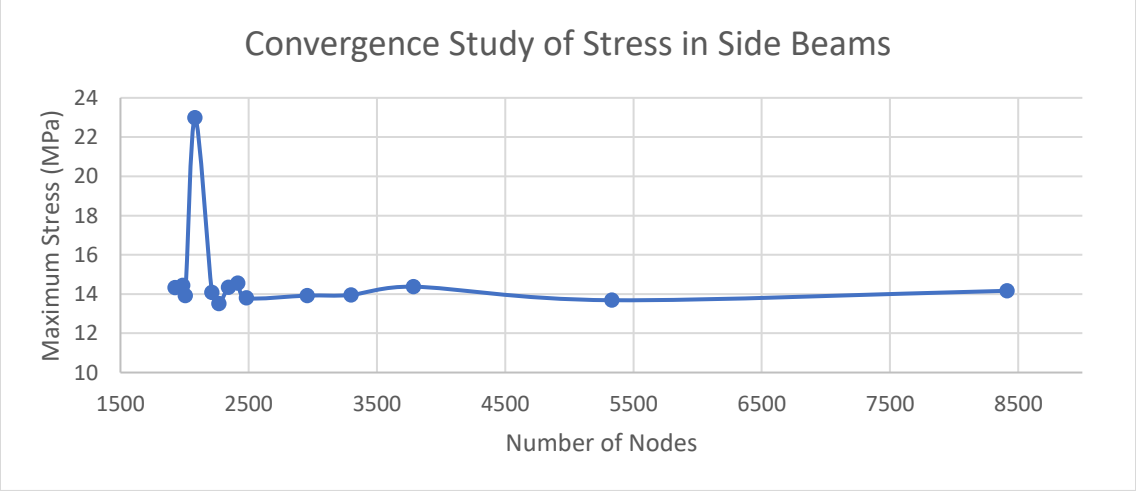

Figure B-2: Side beam convergence plot

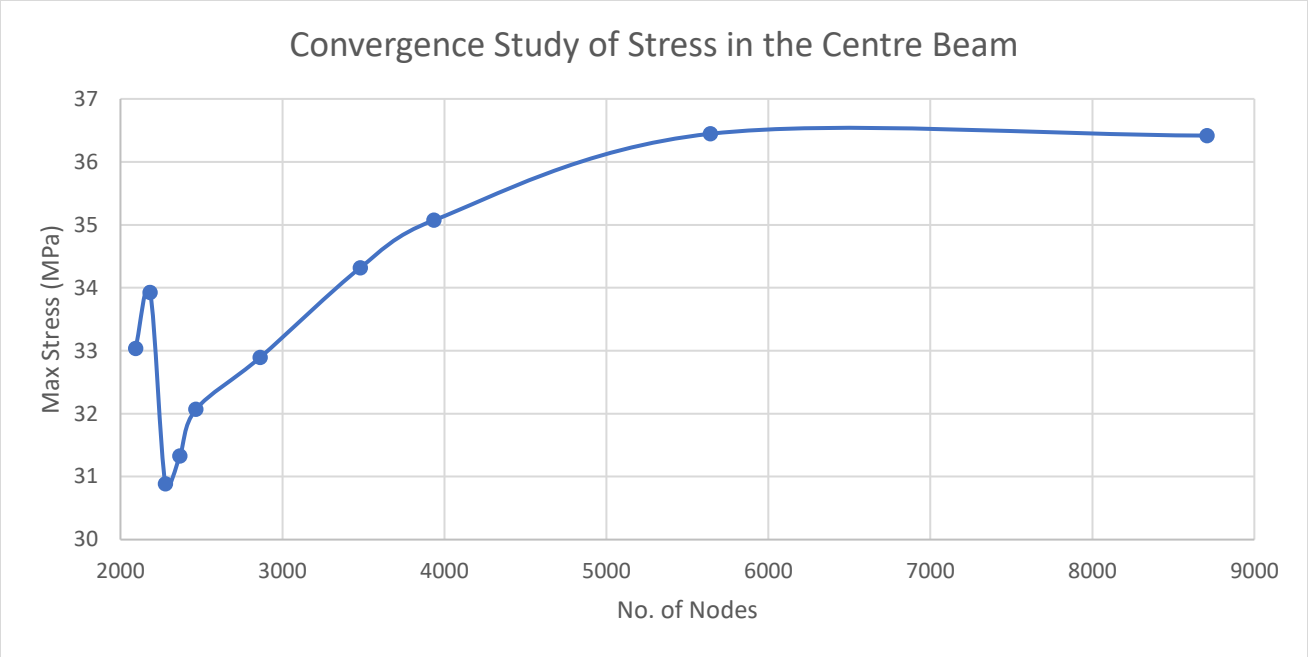

Figure B-3: Center beam convergence plot

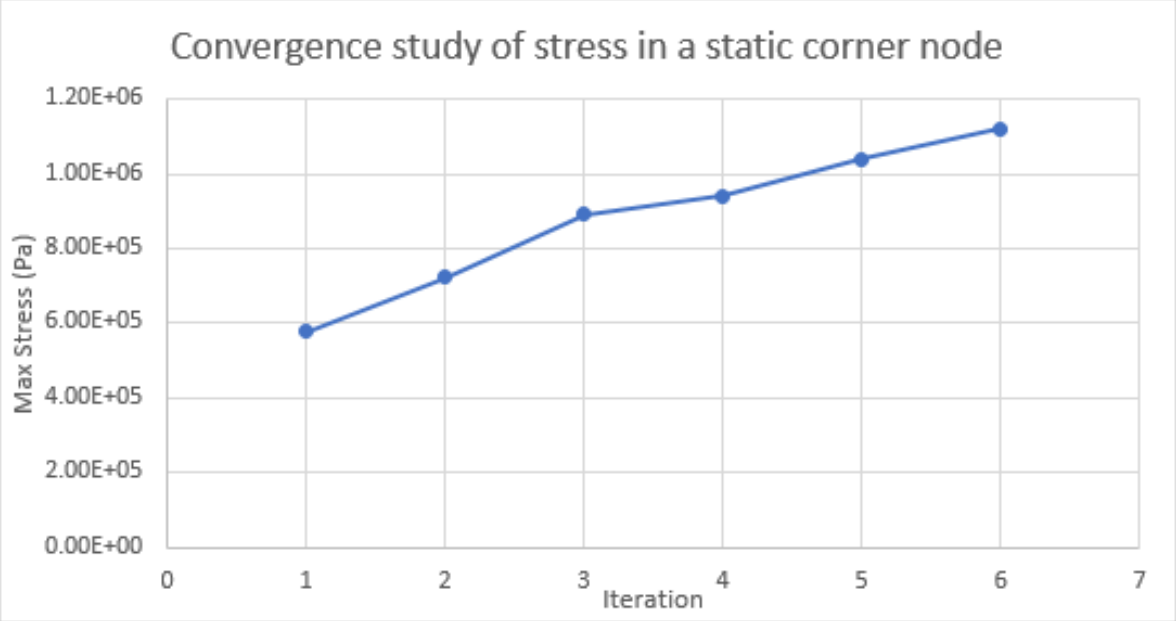

Figure B-4: Corner node static convergence plot

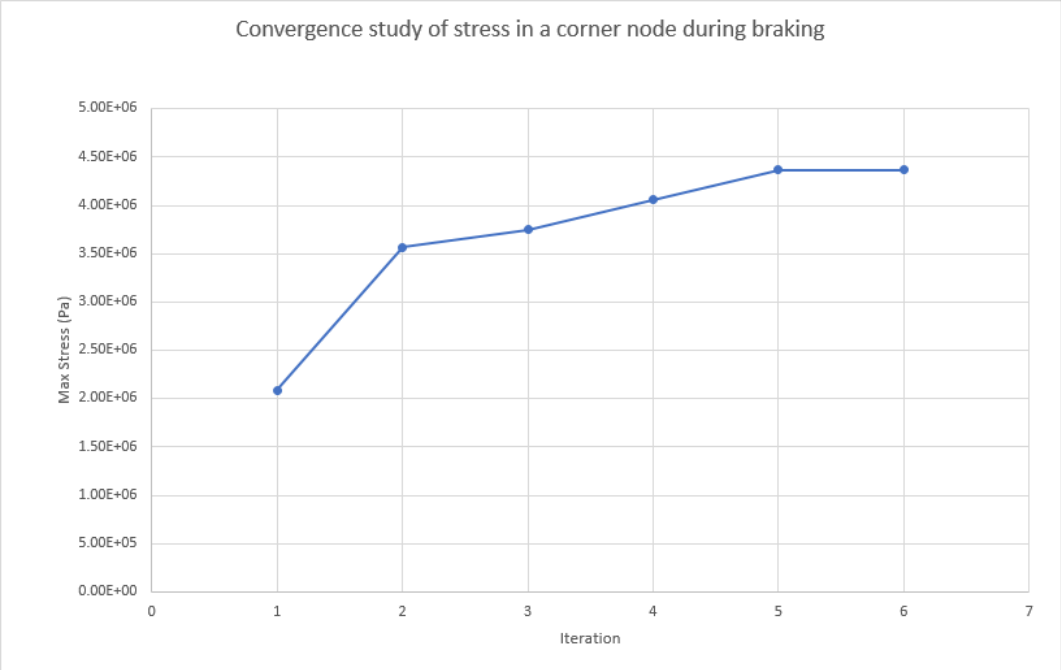

Figure B-5: Corner node braking convergence plot

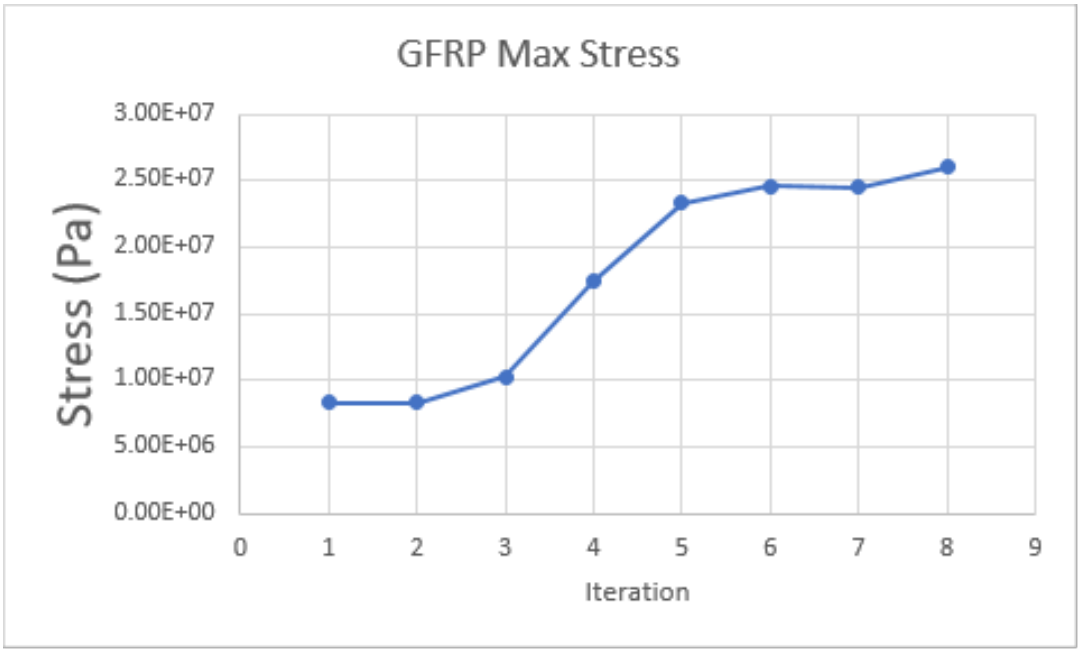

Figure B-6: Walkway max stress convergence plot

Appendix C – FEA Beam Loading Conditions

The loading conditions of the front, side, and center beams are summarized in this appendix. The following is the list of beams as well as their respective figures:

- Front Beam – Figure C-1
- Side Beam – Figure C-2
- Center Beam – Figure C- 3

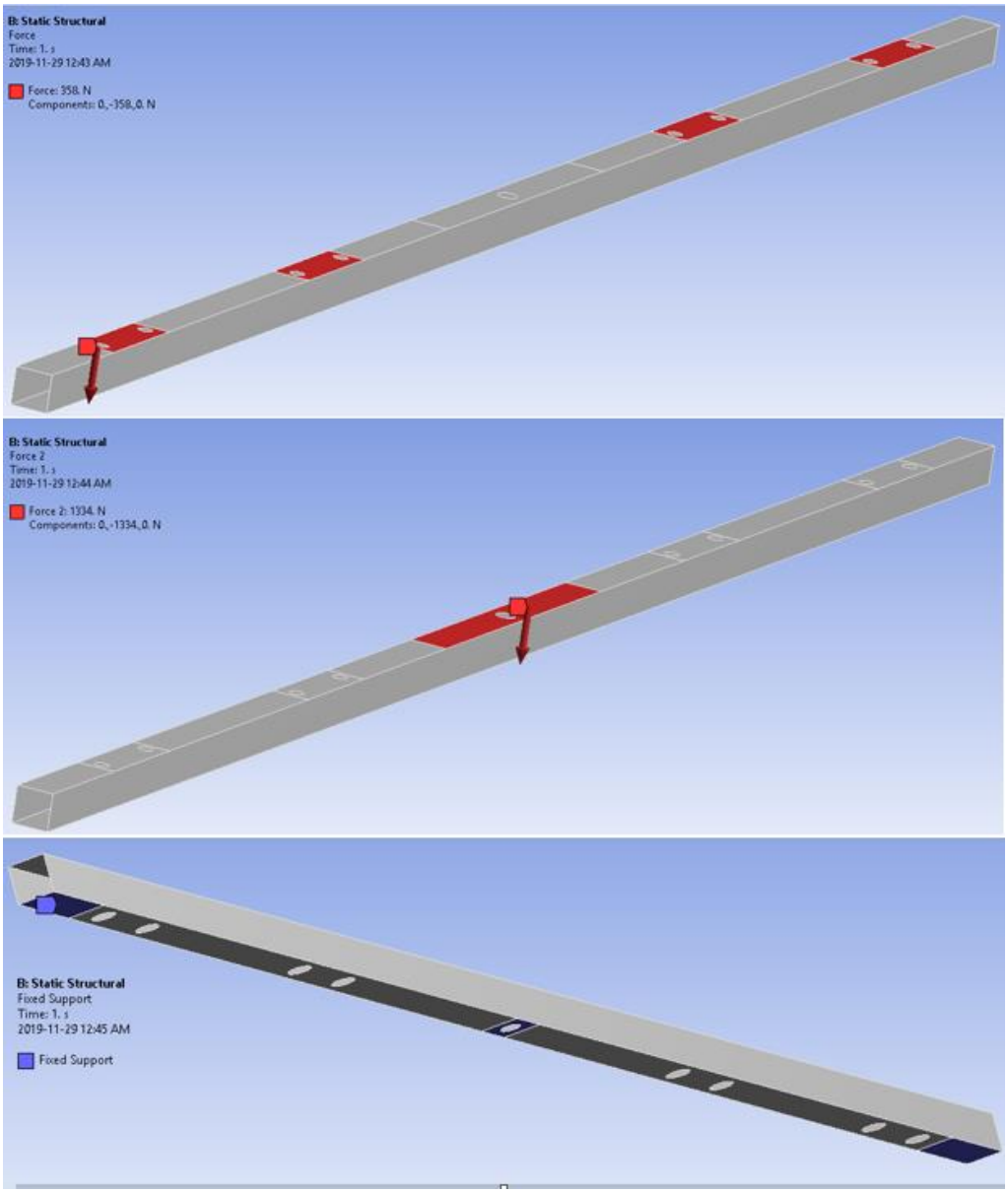

Figure C-1: Front beam loading conditions

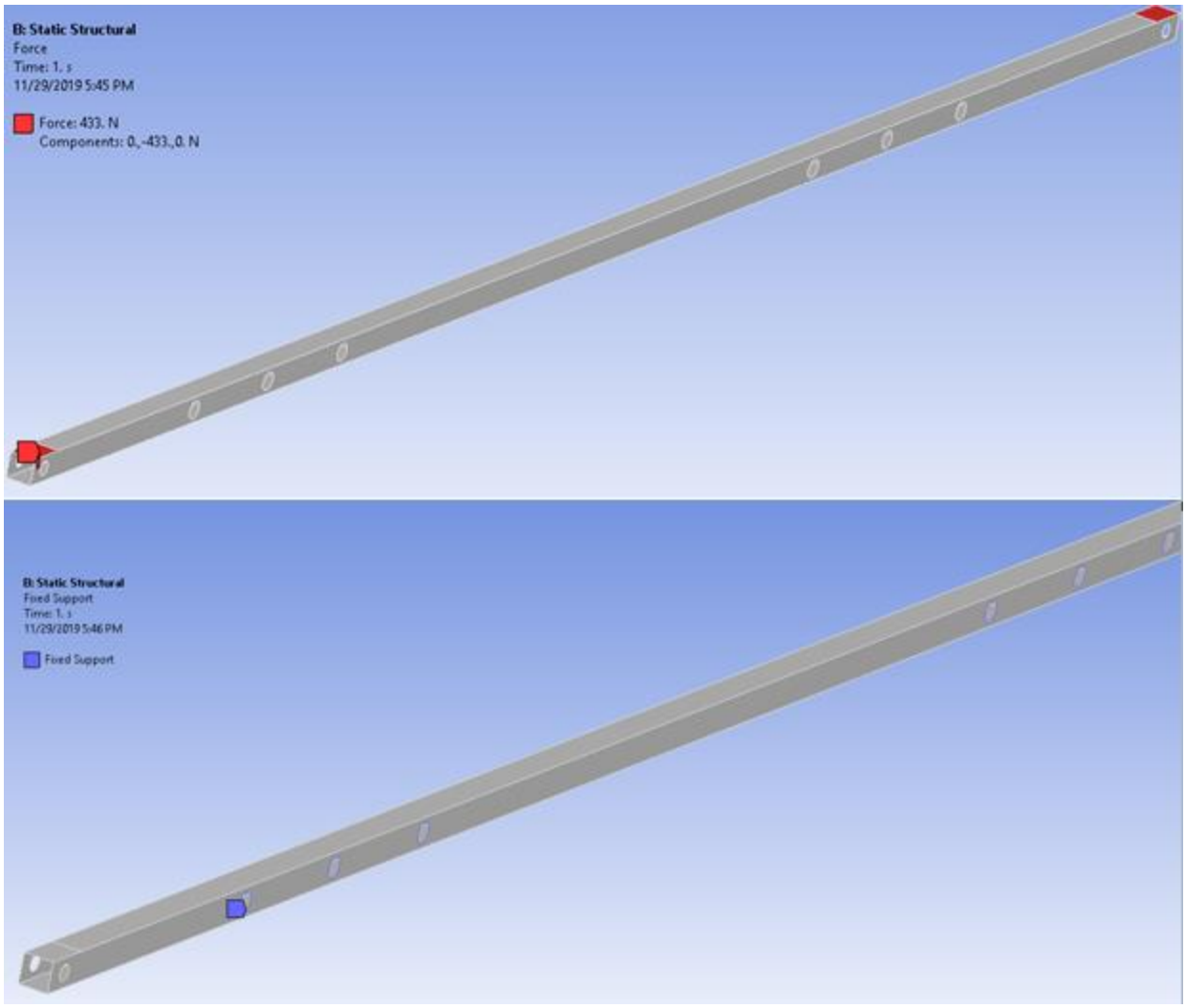

Figure C-2: Side beam loading conditions

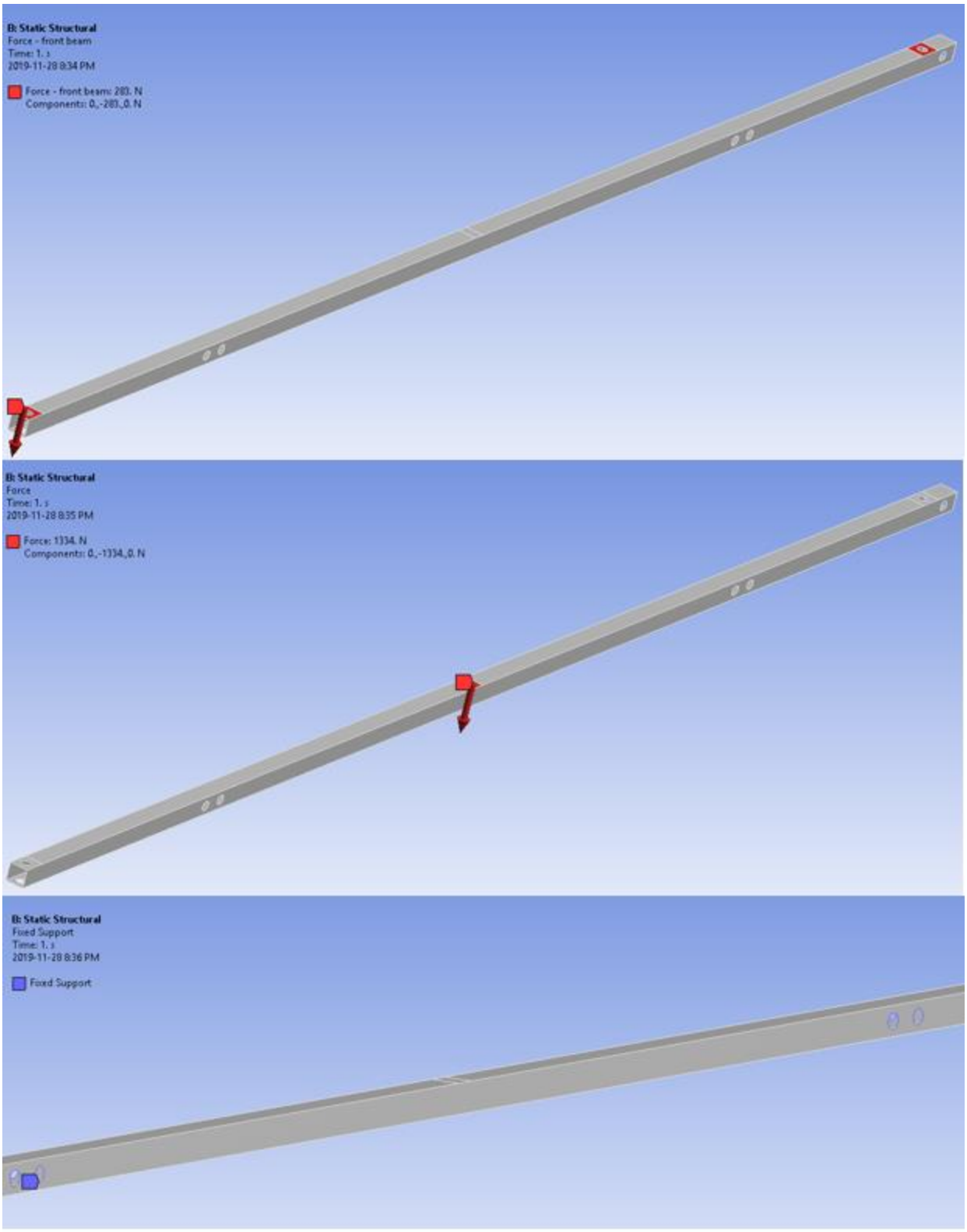

Figure C- 3: Center beam loading condition

Appendix D – Ansys Beam Pre-ACP Composite Settings

The beams were given their material by using Pre-ACP in Ansys to establish composite ply orientation. This appendix gives the settings which the beams used for their analysis. The following list details which settings are shown in which figure:

- Fabric settings – Figure D- 1
- Stackup settings – Figure D- 2
- Rosette settings – Figure D- 3
- Oriented selection set settings – Figure D- 4
- Modelling ply settings - Figure D- 5

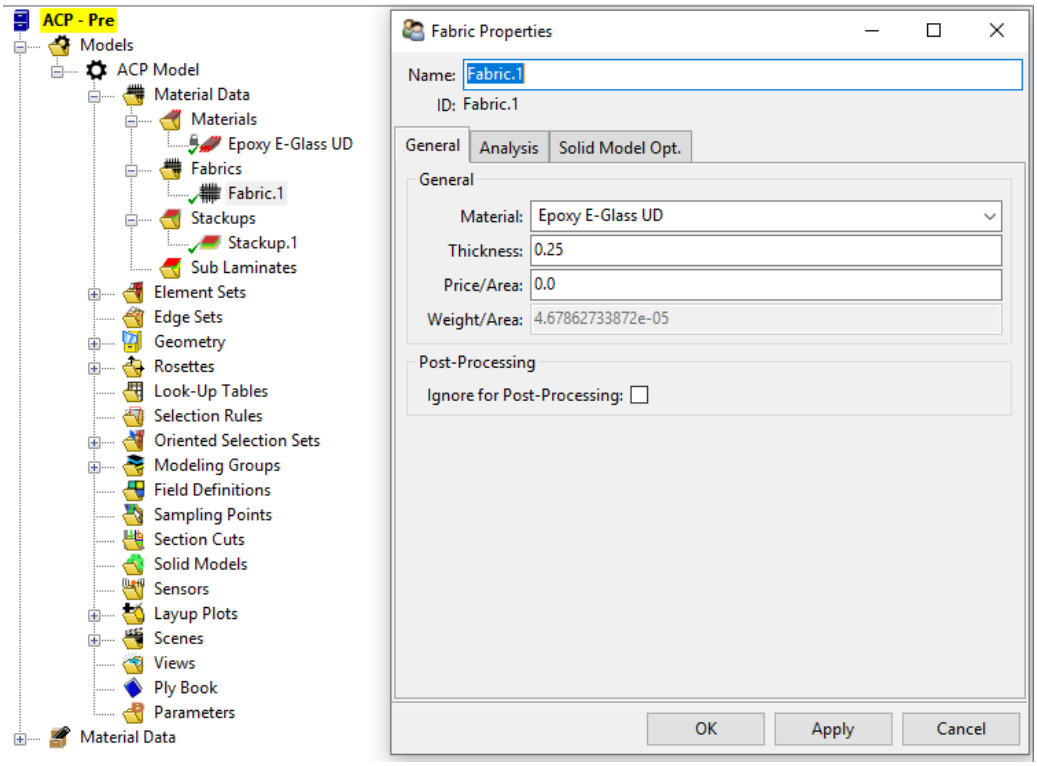

Figure D- 1: Fabric settings

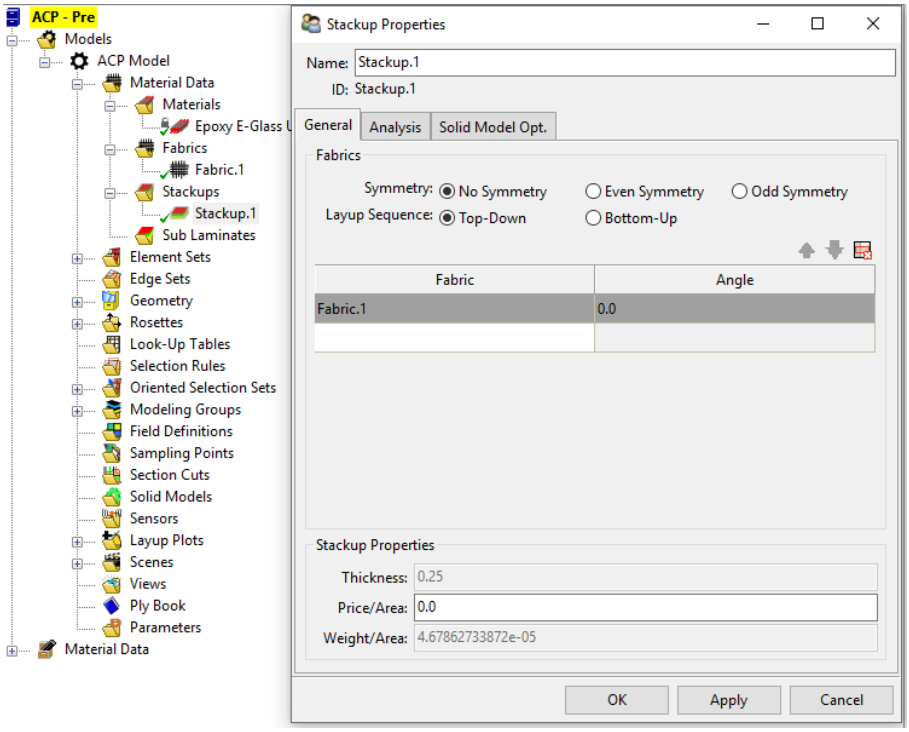

Figure D- 2: Stackup settings

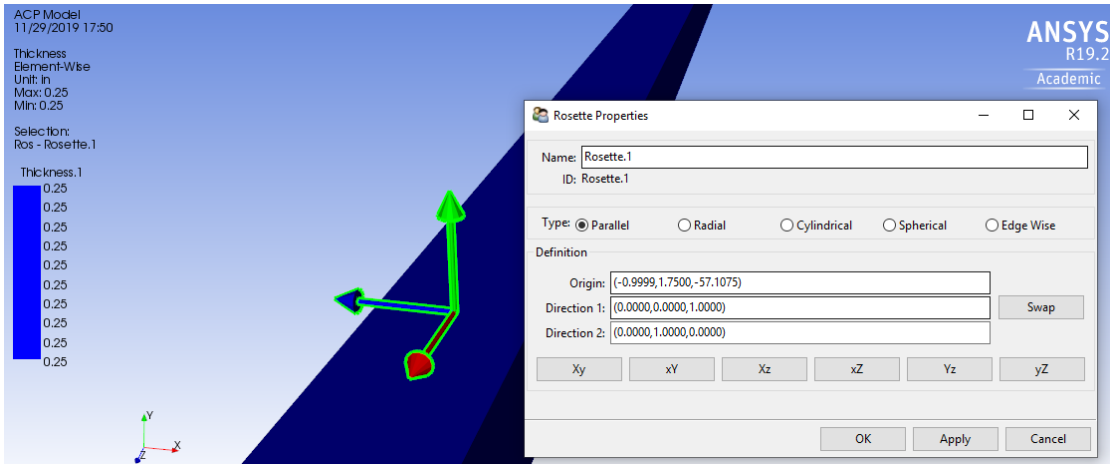

Figure D- 3: Rosette settings

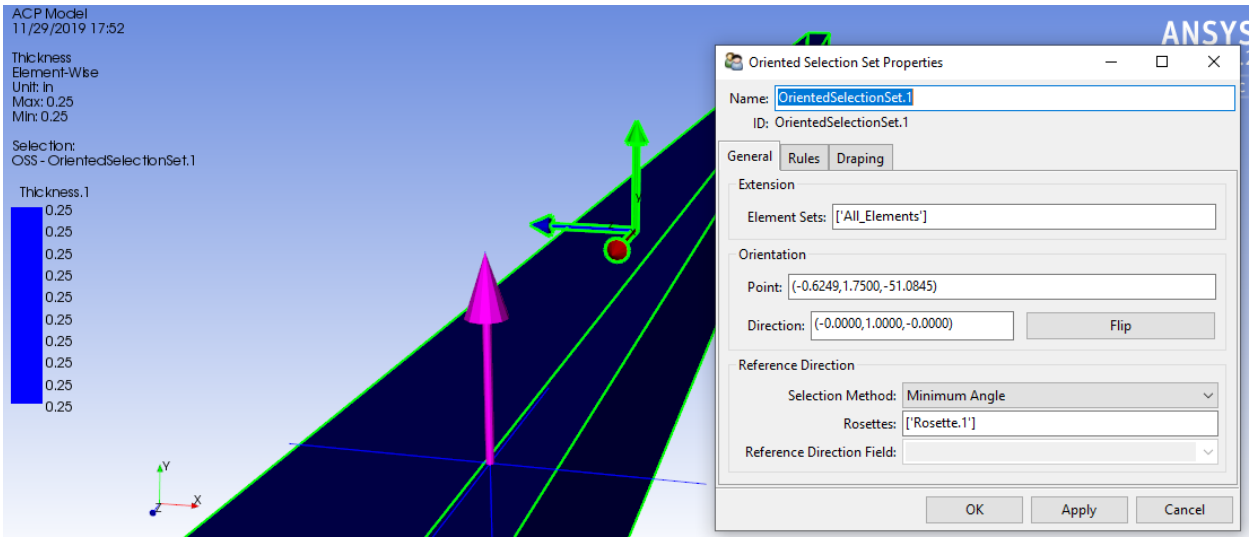

Figure D- 4: Oriented selection set settings

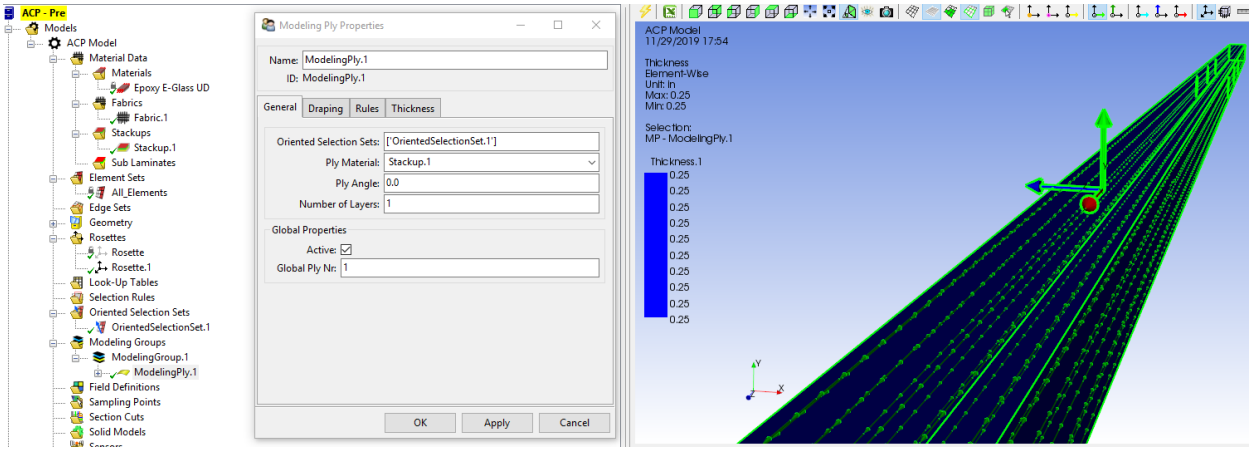

Figure D- 5: Modeling ply settings

Appendix E – Sandwich Analysis Spreadsheet

The calculations of deciding the thickness of each laminate are based on equation 20, the core thickness is ranging from 0.01in to 1.5in, and the corresponding skin thickness is calculated though Microsoft Excel, the input data and a section of the spreadsheet is shown in Figure E- 1.

	1	2	3	4
	gfrp-balsa-gfrp	Al-Corecell A500-Al	Al-Pxc.245-Al	cf-balsa-cf
Ef (Msi)	10.3	10	10	30
ρf(lb/in3)	0.092	0.098	0.098	0.065
ρs(ρc*)	0.0034	0.0034	0.09	0.0034
Ec (Es)	0.289	0.0093	0.08	0.289
Gc* (Msi)	0.1156	0	0	0.1156

B1	B2	B3	B4	C1	C2
76.8	8	2	1	1	0.4

	length L (in)	width b (in)
uniform load	14	126

δ - Max.deflection (in)	P-Applied Force (lbf	δ/P
0.0625	300	0.000208

Figure E- 1: Skin thickness input data

The results of the spreadsheet can be seen in Figure E- 2.

					skin thick		
core thick				t/L	t	total thick	weight
c	C/L			0.200675	2.809451	5.628901	911.9402
0.01	0.000714			0.048677	0.681474	1.382949	221.3101
0.02	0.001429			0.021422	0.299904	0.629809	97.52169
0.03	0.002143			0.011991	0.167872	0.375745	54.72722
0.04	0.002857			0.007652	0.107124	0.264249	35.06987
0.05	0.003571			0.005303	0.074247	0.208495	24.45874
0.06	0.004286			0.003891	0.054473	0.178947	18.10058
0.07	0.005			0.002976	0.041663	0.163326	14.00257
0.08	0.005714			0.002349	0.032892	0.155784	11.21581
0.09	0.006429			0.001902	0.026625	0.153251	9.241756
0.1	0.007143			0.001571	0.021993	0.153986	7.798111
0.11	0.007857			0.001319	0.018472	0.156944	6.715292
0.12	0.008571			0.001124	0.015734	0.161467	5.886448
0.13	0.009286			0.000969	0.013562	0.167124	5.241539
0.14	0.01			0.000844	0.011811	0.173621	4.733103
0.15	0.010714			0.000741	0.010378	0.180756	4.328057
0.16	0.011429			0.000656	0.009191	0.188382	4.002765
0.17	0.012143			0.000585	0.008197	0.196393	3.739981
0.18	0.012857			0.000525	0.007355	0.20471	3.526879
0.19	0.013571			0.000474	0.006637	0.213274	3.353761
0.2	0.014286			0.00043	0.006019	0.222038	3.213187
0.21	0.015			0.000392	0.005484	0.230968	3.099368
0.22	0.015714			0.000358	0.005017	0.240033	3.007749
0.23	0.016429			0.000329	0.004607	0.249214	2.934703
0.24	0.017143			0.000303	0.004245	0.258491	2.877316
0.25	0.017857			0.00028	0.003925	0.267849	2.833223
0.26	0.018571			0.00026	0.003639	0.277278	2.80049
0.27	0.019286			0.000242	0.003383	0.286767	2.777522
0.28	0.02			0.000225	0.003154	0.296308	2.762993
0.29	0.020714			0.00021	0.002947	0.305894	2.755797
0.3	0.021429			0.000197	0.00276	0.315519	2.755002
0.31	0.022143			0.000185	0.00259	0.32518	2.759819
0.32	0.022857			0.000174	0.002435	0.33487	2.769579
0.33	0.023571			0.000164	0.002294	0.344588	2.783708
0.34	0.024286			0.000155	0.002165	0.354329	2.801714
0.35	0.025			0.000146	0.002046	0.364092	2.82317

Figure E- 2: Results of the thickness calculations